



**HAL**  
open science

## Mutant mice lacking alternatively spliced p53 isoforms unveil Akr4 as a male-specific prognostic factor in Myc-driven B-cell lymphomas

Anne Fajac, Iva Simeonova, Julia Leemput, Marc Gabriel, Aurélie Morin, Vincent Lejour, Annaïg Hamon, Jeanne Rakotopare, Wilhelm Vaysse-Zinkhöfer, Eliana Eldawra, et al.

### ► To cite this version:

Anne Fajac, Iva Simeonova, Julia Leemput, Marc Gabriel, Aurélie Morin, et al.. Mutant mice lacking alternatively spliced p53 isoforms unveil Akr4 as a male-specific prognostic factor in Myc-driven B-cell lymphomas. *eLife*, 2024, 13, 10.7554/eLife.92774 . hal-04717438

**HAL Id: hal-04717438**

**<https://hal.science/hal-04717438v1>**

Submitted on 6 Jan 2025

**HAL** is a multi-disciplinary open access archive for the deposit and dissemination of scientific research documents, whether they are published or not. The documents may come from teaching and research institutions in France or abroad, or from public or private research centers.

L'archive ouverte pluridisciplinaire **HAL**, est destinée au dépôt et à la diffusion de documents scientifiques de niveau recherche, publiés ou non, émanant des établissements d'enseignement et de recherche français ou étrangers, des laboratoires publics ou privés.



Distributed under a Creative Commons Attribution 4.0 International License

# Mutant mice lacking alternatively spliced p53 isoforms unveil *Ackr4* as a male-specific prognostic factor in Myc-driven B-cell lymphomas

## Reviewed Preprint

Published from the original preprint after peer review and assessment by eLife.

## About eLife's process

## Reviewed preprint version 1



January 10, 2024 (this version)

## Posted to preprint server

October 18, 2023

## Sent for peer review

October 13, 2023

Anne Fajac, Iva Simeonova, Julia Leemput, Marc Gabriel, Aurélie Morin, Vincent Lejour, Annaïg Hamon, Wilhelm Vaysse-Zinkhöfer, Eliana Eldawra, Jeanne Rakotopare, Marina Pinskaya, Antonin Morillon, Jean-Christophe Bourdon, Boris Bardot , Franck Toledo 

Genetics of Tumor Suppression, Institut Curie, Paris, 75248 Cedex 05, France • CNRS UMR3244, Paris, France • Sorbonne University, Paris, France • PSL Research University, Paris, France • Non Coding RNA, Epigenetic and Genome Fluidity, Institut Curie, Paris, France • Ninewells Hospital, University of Dundee, Dundee 195Y, Scotland

 [https://en.wikipedia.org/wiki/Open\\_access](https://en.wikipedia.org/wiki/Open_access)

 Copyright information

## Abstract

The gene encoding p53, a major tumor suppressor protein, encodes several alternative isoforms of elusive biological significance. Here we show that mice lacking the *Trp53* Alternatively Spliced (AS) exon, thereby expressing the canonical p53 protein but not isoforms with the AS C-terminus, have unexpectedly lost a male-specific protection against Myc-induced B-cell lymphomas. Lymphomagenesis was delayed in p53<sup>+/+</sup> Eμ-Myc males compared to p53<sup>ΔAS/ΔAS</sup> Eμ-Myc males, but also compared to p53<sup>+/+</sup> Eμ-Myc and p53<sup>ΔAS/ΔAS</sup> Eμ-Myc females. Pre-tumoral splenocytes from p53<sup>+/+</sup> Eμ-Myc males exhibited a higher expression of *Ackr4*, encoding an atypical chemokine receptor with tumor suppressive effects. We show that *Ackr4* is a p53 target gene, but that its p53-mediated transactivation is inhibited by estrogens. We identify *Ackr4* as a male-specific factor of good prognosis, relevant for murine Eμ-Myc-induced and human Burkitt lymphomas. These data demonstrate the functional relevance of alternatively spliced p53 isoforms and reveal sex disparities in Myc-driven B-cell lymphomagenesis.

### eLife assessment

This **important** study using engineered mouse models provides a first **compelling** demonstration of a pathogenic phenotype associated with lack of expression of p53AS, an isoform of the p53 protein with a different C-terminus as canonical p53. The work also offers correlative evidence that *Ackr4*, differentially expressed in this mouse model, may be a male-specific prognostic factor in a specific type of B-cell lymphomas. Direct functional evidence testing the links proposed would better support the major findings of the study.

## Introduction

*TP53*, the human gene for tumor suppressor p53, encodes several isoforms owing to distinct promoters, alternative splicing and multiple translation initiation sites (Bourdon et al., 2005; Courtois et al., 2002; Flaman et al., 1996; Yin et al., 2002). p53 alternative isoforms can be abnormally expressed in cancer cells and some may regulate the canonical p53 protein (Anbarasan and Bourdon, 2019; Bourdon et al., 2005; Mondal et al., 2013; Senturk et al., 2014). However, aberrant RNA splicing is a common feature of cancer cells (Graubert et al., 2012; Martin et al., 2013; Pajares et al., 2007; Sette and Paronetto, 2022) and to which extent alternative splicing generates functionally relevant proteins is controversial (Abascal et al., 2015; Blencowe, 2017; Tress et al., 2017a, 2017b; Ule and Blencowe, 2019; Weatheritt et al., 2016). Thus, the biological importance of many p53 isoforms remains elusive.

Like its human *TP53* homolog, the murine *Trp53* gene encodes multiple isoforms differing in their N- or C-termini (Arai et al., 1986; Marcel et al., 2011). Mouse models to evaluate the role of p53 isoforms differing in their N-terminus revealed that  $\Delta 40$ -p53 overexpression leads to accelerated ageing (Maier et al., 2004; Steffens Reinhardt et al., 2020). However, the potential role of p53 isoforms with an alternative C-terminus was not analyzed *in vivo*. p53 isoforms with distinct C-termini result from the splicing of two mutually exclusive final exons: exon 11, encoding the canonical “ $\alpha$ ” C-terminal domain, and the Alternatively Spliced (AS) exon, encoding another C-terminus (Arai et al., 1986). In adult mice, isoforms with the canonical C-terminus are predominant in all tissues (Figure S1A). Two models (p53 <sup>$\Delta 31$</sup>  and p53 <sup>$\Delta$ CTD</sup>), designed to study the consequences of a loss of the canonical p53 C-terminus, exhibited signs of increased p53 activity leading to a rapidly lethal anemia (Hamard et al., 2013; Simeonova et al., 2013). To determine the role of p53-AS isoforms *in vivo*, we created p53 <sup>$\Delta$ AS</sup>, a mouse model with a specific deletion of the AS exon (Figure S1B). In mouse embryonic fibroblasts (MEFs), the *Trp53* <sup>$\Delta$ AS</sup> allele prevented the expression of isoforms with the AS C-terminus whereas it did not affect RNA levels for p53 isoforms with the canonical C-terminus (Figure S1C). We previously used this model to show that p53-AS isoforms had no role in the anemia affecting p53 <sup>$\Delta 31/\Delta 31$</sup>  mice (Simeonova et al., 2013). However, a detailed phenotyping of p53 <sup>$\Delta$ AS/ $\Delta$ AS</sup> mice remained to be performed. The detailed phenotyping, presented here, yielded surprising information on lymphomagenesis.

## Results

### Stress responses in WT and p53 <sup>$\Delta$ AS/ $\Delta$ AS</sup> cells

Thymocytes undergo a p53-dependent apoptosis upon irradiation (Lowe et al., 1993). We analyzed thymocytes from irradiated wild-type (WT) and p53 <sup>$\Delta$ AS/ $\Delta$ AS</sup> mice. In WT thymocytes, isoforms with the AS C-terminus were 5 times less abundant than isoforms with the  $\alpha$  C-terminus at the RNA level (Figure 1A), and in western blots the p53-AS protein appeared as a faint band running just ahead of, and often hard to separate from, the band specific for p53- $\alpha$ , the canonical full-length p53 (Figure 1B). In p53 <sup>$\Delta$ AS/ $\Delta$ AS</sup> thymocytes, mRNA levels for  $\alpha$  isoforms were slightly decreased, if at all (Figure 1A), whereas p53- $\alpha$  protein levels appeared markedly decreased (Figure 1B), raising the possibility that p53-AS isoforms might contribute to p53- $\alpha$  abundance. Nevertheless, the transactivation of classical p53 target genes (Figure 1C) and apoptotic response (Figures 1D and S1D) were not significantly altered by the loss of AS isoforms. Likewise, no significant difference was observed between WT and p53 <sup>$\Delta$ AS/ $\Delta$ AS</sup> fibroblasts in assays for cell cycle control (Figures 1E and S1E), expression of well-known p53 target genes (Figure 1F and S1F-G), proliferation under hyperoxic conditions (Figure 1G), or the growth of tumor xenografts (Figure 1H).

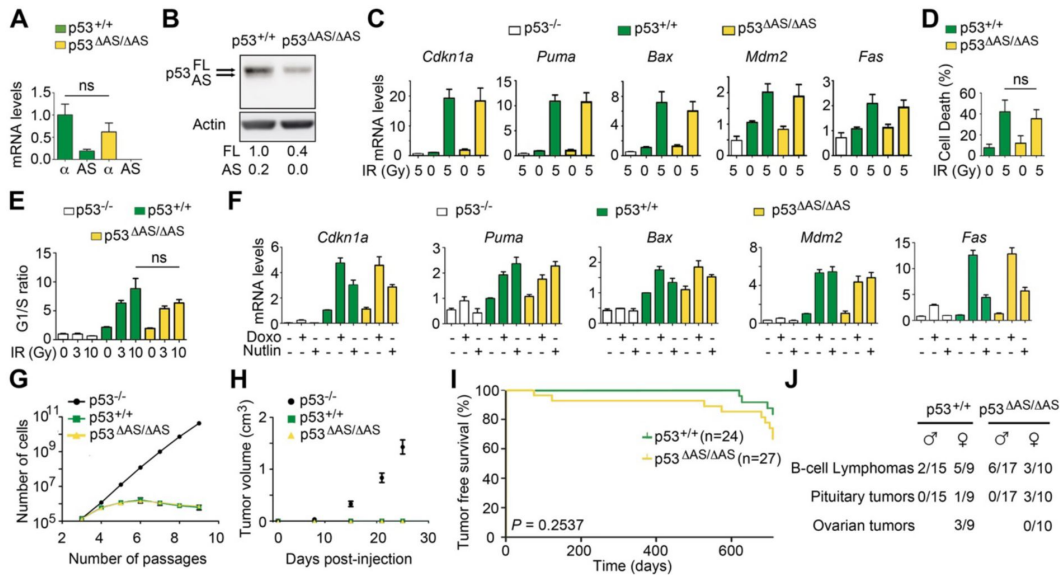


**Figure 1.**

**The loss of p53-AS isoforms does not alter cellular stress responses or survival to spontaneous tumors.**

(A) mRNAs for p53-α and p53-AS isoforms from thymocytes of irradiated mice were quantified by RT-qPCR, and p53-α levels in p53<sup>+/+</sup> mice were assigned a value of 1. Means ± SEM (n=3). (B) Protein extracts from thymocytes of irradiated mice were immunoblotted with p53 or actin antibodies. After normalisation to actin, full-length (FL) p53-α levels in p53<sup>+/+</sup> thymocytes were assigned a value of 1. (C) mRNA levels of p53 target genes in thymocytes, before or after ψ-irradiation. Means ± SEM (n=3). (D) Thymocyte apoptotic response to ψ-irradiation. Means ± SEM (n=6). (E) Cell cycle control in mouse embryonic fibroblasts (MEFs) after ψ-irradiation. Asynchronous MEFs were exposed to 0-10 Gy ψ-irradiation, and after 24 hr, cells were labelled with BrdU for 1 hr and analyzed by FACS. Means ± SEM from >3 independent experiments with at least 2 independent MEF clones per genotype. (F) mRNA levels of p53 target genes in MEFs untreated or treated with 0.5 μg/ml of clastogenic Doxorubicin (Doxo) or 10 μM of the Mdm2 antagonist Nutlin. Means ± SEM from > 3 experiments with ≥ 2 independent MEF clones. (G) MEFs proliferation under hyperoxic conditions. Cells were grown according to a 3T3 protocol. Each point is the mean from 4 independent MEF clones, the value for each clone resulting from triplicates. (H) Growth of tumor xenografts. E1A+Ras-expressing MEFs were injected into the flanks of nude mice and tumor volumes were determined after 1-25 days. Means ± SD (n=4 per timepoint and genotype). (I) Tumor-free survival of p53<sup>+/+</sup> and p53<sup>ΔAS/ΔAS</sup> mice (n=cohort size). (J) Incidence of the indicated tumor types, determined at death after macroscopic examination and histological analysis. In A, D, E, ns=non-significant in Student's t-test.

## Lymphomagenesis in WT and p53<sup>ΔAS/ΔAS</sup> mice

We compared spontaneous tumor onset in WT and p53<sup>ΔAS/ΔAS</sup> littermates for over 2 years and observed no significant difference in tumor-free survival (**Figure 1I**). Because lymphoma is a common neoplasm in C57BL6/J WT mice (Brayton et al., 2012) and our mouse cohorts resulted from >10 generations of backcrosses with C57BL6/J mice, we searched for evidence of lymphoma in the lymph nodes and spleen, by macroscopic examination at autopsy and histological analyses. B-cell lymphomas were observed in about 30% of mice of either genotype (**Figure 1J**). In p53<sup>+/+</sup> mice, a higher incidence of B-cell lymphomas was observed in females, in agreement with previous observations (Brayton et al., 2012). By contrast, no obvious sex-specific bias was observed for B-cell lymphomas in p53<sup>ΔAS/ΔAS</sup> mice (**Figure 1J**), raising the possibility that the loss of p53-AS isoforms affected B-cell lymphomagenesis. However, the numbers of lymphoma-bearing mice were too small to be conclusive.

We next used Eμ-Myc transgenic mice, prone to highly penetrant B-cell lymphomas (Adams et al., 1985). p53<sup>+/+</sup> Eμ-Myc and p53<sup>ΔAS/ΔAS</sup> Eμ-Myc mice developed B-cell lymphomas (Figure S2A) with similar survival curves when sexes were not considered (Figure S2B). Importantly however, death was accelerated, and tumor lymph nodes were larger, in p53<sup>ΔAS/ΔAS</sup> Eμ-Myc males compared to their p53<sup>+/+</sup> Eμ-Myc male counterparts, whereas no difference in lymphomagenesis was noticeable between p53<sup>ΔAS/ΔAS</sup> Eμ-Myc and p53<sup>+/+</sup> Eμ-Myc female mice (**Figure 2A-B**). Our data (**Figures 2A-B** and S2C), together with the fact that B-cell lymphomas occur with a higher incidence in WT C57BL6/J female mice (Brayton et al., 2012), suggested that p53<sup>+/+</sup> Eμ-Myc male mice are more refractory to B-cell lymphomas, and that p53-AS isoforms might confer this male-specific protection against lymphomagenesis.

## Cause for accelerated lymphomagenesis in p53<sup>ΔAS/ΔAS</sup> Eμ-Myc males

We next aimed to determine the mechanisms underlying the accelerated lymphomagenesis in p53<sup>ΔAS/ΔAS</sup> Eμ-Myc males. Inactivating p53 mutations were not more frequent in tumors from p53<sup>ΔAS/ΔAS</sup> Eμ-Myc males than in those from p53<sup>+/+</sup> Eμ-Myc males, ruling out additional mutations at the *Trp53* locus as potential causes for accelerated lymphomagenesis in p53<sup>ΔAS/ΔAS</sup> Eμ-Myc males (Figures S2D-E). We next analyzed a subset of tumors with no detectable *Trp53* mutation in males of both genotypes, and found that Myc was expressed at similar RNA and protein levels in all tumors (**Figure 2C**). No difference in p53-α mRNA levels was observed in tumors from both genotypes, although a decrease at the protein level was detected in most tumors from p53<sup>ΔAS/ΔAS</sup> Eμ-Myc males (**Figure 2D**). Nevertheless, similar transcript levels for classical p53 target genes were observed in tumor cells of both genotypes (**Figure 2E**). To test whether a higher tumor volume in p53<sup>ΔAS/ΔAS</sup> Eμ-myc males might result from lower apoptosis and/or higher cell proliferation, we next analyzed tumors by immunohistochemistry with antibodies against cleaved caspase-3 or ki-67, respectively. Similar apoptotic and proliferation indexes were observed for both genotypes (**Figure 2F-G**). In sum, classical assays for p53 activity in tumors failed to account for differences between the two male genotypes.

The speed of lymphomagenesis in Eμ-Myc mice correlates with the extent of B-cell expansion in the first stages of B cell differentiation (Langdon et al., 1986) and p53 was proposed to control the pool of early B cells (Slatter et al., 2010). Therefore, we determined the levels of the early pre-B / immature B cells in 6 weeks-old mice, before any sign of tumor. We analyzed the spleen, a preferential site of B-cell expansion (Langdon et al., 1986) with a relatively high AS/α isoform ratio (Figure S1A). Flow cytometry with a combination of markers was used to discriminate the pre-B, immature, transitional and mature B subpopulations. As expected (Langdon et al., 1986), we observed high numbers of pre-B and immature B cells in Eμ-Myc mice. In males, pre-B and immature B cells were more abundant in p53<sup>ΔAS/ΔAS</sup> Eμ-Myc animals, while no difference was

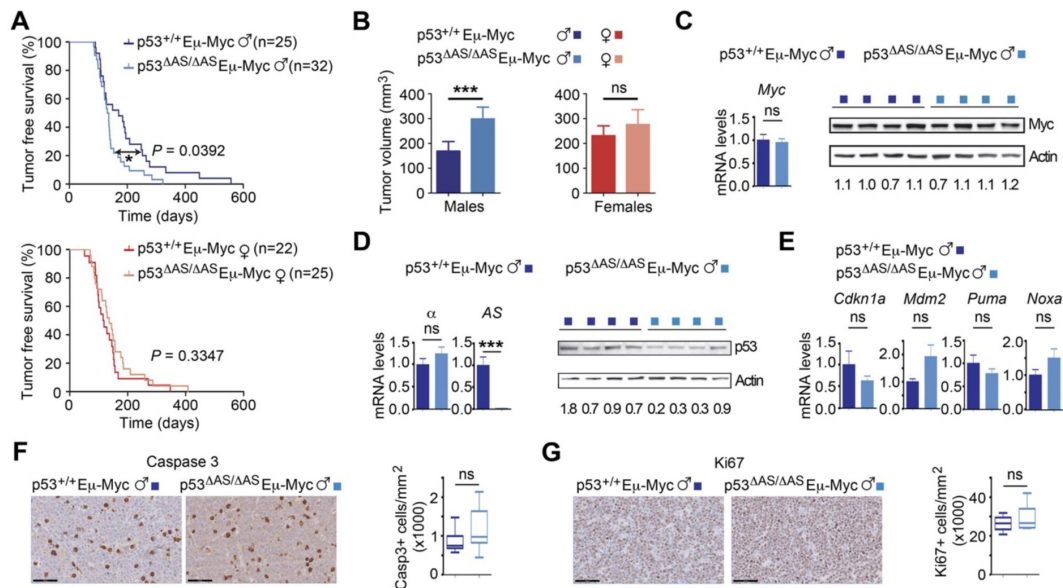


**Figure 2.**

### Male-specific acceleration of Myc-induced B-cell lymphomagenesis in mice lacking p53-AS isoforms.

(A) Tumor-free survival of p53<sup>+/+</sup>Eμ-Myc and p53<sup>ΔAS/ΔAS</sup>Eμ-Myc mice, classified according to sex. (n=cohort size). (B) Tumor volumes upon dissection of p53<sup>+/+</sup>Eμ-Myc and p53<sup>ΔAS/ΔAS</sup>Eμ-Myc mice, classified according to sex. Means ± SEM from 100 lymph nodes from p53<sup>+/+</sup>Eμ-Myc males, 96 from p53<sup>+/+</sup>Eμ-Myc females, 148 from p53<sup>ΔAS/ΔAS</sup>Eμ-Myc males and 124 from p53<sup>ΔAS/ΔAS</sup>Eμ-Myc females. (C) Myc mRNA and protein levels in lymph node tumors. (D) Levels of p53-α and p53-AS transcripts and p53 protein levels in lymph node tumors. (E) Transcript levels of the indicated p53 target genes. Means ± SEM (n=6 per genotype). (F-G) Apoptosis (F) and cell proliferation (G) in tumor lymph nodes from Eμ-Myc males were determined by immunohistochemistry with antibodies against cleaved caspase-3 and ki67, respectively. Positive cells were counted and normalized to the analyzed areas. Means ± SEM (n=6 mice per assay and genotype). In F, G scale bars=50 μm. Statistical analyses with Mantel-Cox (A) and Student's t (B-G) tests. \*\*\*P<0.001, \*P<0.05, ns: non-significant.



observed for transitional and mature B cells (**Figures 3A** and S3A). By contrast, in the spleen of  $p53^{+/+}$  and  $p53^{\Delta AS/\Delta AS}$  6 weeks-old male mice without the E $\mu$ -Myc transgene, most B cells were mature B cells (Figure S3B). In E $\mu$ -Myc females, the numbers of pre-B and immature B cells were similar between genotypes, as were the numbers of transitional and mature B cells (**Figure 3A**). Interestingly,  $p53^{+/+}$  E $\mu$ -myc males, which develop lymphomas less rapidly, exhibited the lowest number of immature B cells (**Figure 3A**), suggesting a direct correlation between the level of immature B cell expansion and the speed of lymphomagenesis. Together, these data suggested that p53-AS isoforms may not be required to control the pool of early B cells under normal conditions, but that in an E $\mu$ -Myc context they would limit the expansion of pre-tumor early B cells, specifically in males.

## Transcriptomes from $p53^{+/+}$ E $\mu$ -Myc and $p53^{\Delta AS/\Delta AS}$ E $\mu$ -Myc male spleens

We next performed bulk RNA-seq and differential expression analyses comparing the spleens from 4-6 weeks-old  $p53^{\Delta AS/\Delta AS}$  E $\mu$ -Myc males to spleens from age-matched  $p53^{+/+}$  E $\mu$ -Myc males. This revealed a limited number of significantly deregulated genes (**Figure 3B**), including 13 protein-coding genes and 11 pseudogenes (**Figure 3C**). Out of the 13 protein-coding genes, we focused on the 10 genes not encoding an immunoglobulin and analyzed the same samples by RT-qPCR (**Figure 3D**). For 6 of the 10 genes, expression levels were too low to be quantified (*Tcstv3*), or differences in expression were not statistically significant (*Masp2*, *Akr1c19*, *Cd300lh*, *Il5ra*, *Slc26a1*). Of note, *Il5ra* belonged to this group, although it is regulated by p53 (Zhu et al., 2022), which illustrates the difficulty to analyze subtle effects in our experiments. Taking this into account, we considered as potentially interesting the 4 remaining genes, exhibiting differences in mRNA levels with statistical significance ( $p < 0.05$ ) or borderline statistical significance ( $p = 0.057$ ): *Ackr4*, less expressed in  $p53^{\Delta AS/\Delta AS}$  E $\mu$ -Myc males, and *Fam132a*, *Mt2* and *Prss50*, with an increased expression in  $p53^{\Delta AS/\Delta AS}$  E $\mu$ -Myc males (**Figure 3D**). Importantly, survival curves indicated that the Myc-induced lethality was delayed in  $p53^{+/+}$  E $\mu$ -Myc males compared to  $p53^{\Delta AS/\Delta AS}$  E $\mu$ -Myc males,  $p53^{+/+}$  E $\mu$ -Myc females and  $p53^{\Delta AS/\Delta AS}$  E $\mu$ -Myc females (Figure S2C). Thus, we quantified transcripts for *Ackr4*, *Fam132a*, *Mt2* and *Prss50* in the spleen of 4-6 weeks-old  $p53^{+/+}$  E $\mu$ -Myc and  $p53^{\Delta AS/\Delta AS}$  E $\mu$ -Myc females, then compared mRNA levels in  $p53^{+/+}$  E $\mu$ -Myc males versus the 3 other groups. Significantly higher expression of *Ackr4* and lower expression of *Mt2* were found in  $p53^{+/+}$  E $\mu$ -Myc males (**Figure 3E**).

*Ackr4* encodes the atypical chemokine receptor 4, a decoy receptor promoting the degradation of chemokines that modulate cancer cell proliferation and metastasis (Chow and Luster, 2014; Marcuzzi et al., 2018; Müller et al., 2001). Our data suggested that *Ackr4* might be a gene transactivated by p53- $\alpha$  and/or p53-AS isoforms. Consistent with this, by extracting data from a transcriptome-wide study in MEFs (Younger et al., 2015) we found evidence for a p53-dependent transactivation of *Ackr4* in response to doxorubicin (**Figure 3F**). Furthermore, ChIP-Atlas, the database of chromatin immunoprecipitation experiments (Oki et al., 2018), indicated p53 binding to sequences within the intron 1 of *Ackr4* in doxorubicin-treated MEFs, and we identified a candidate p53 responsive element in this intron (**Figure 3G**). We next used luciferase assays to show that this p53 responsive element can be bound and regulated by both p53- $\alpha$  and p53-AS (**Figures 3G-H** and S3C). Together, these data show that *Ackr4* is indeed a p53 target gene, although RNAseq data indicated that it is expressed at much lower levels than classical p53 targets like *Cdkn1a* or *Mdm2* in the splenocytes of E $\mu$ -Myc mice (Table S1). Furthermore, *Ackr4* was shown to be regulated by Foxl2 and estrogen signalling in ovarian cells (Georges et al., 2014) and 17- $\beta$  estradiol was recently found to regulate *ACKR4* expression in meniscal cells from both sexes, albeit differentially (Knewton et al., 2020). Accordingly, we observed, in both WT and  $p53^{\Delta AS/\Delta AS}$  MEFs, that p53 activation with the Mdm2 antagonist Nutlin led to the transactivation of *Ackr4*, but that a concomitant treatment with 17- $\beta$  estradiol markedly decreased, or completely

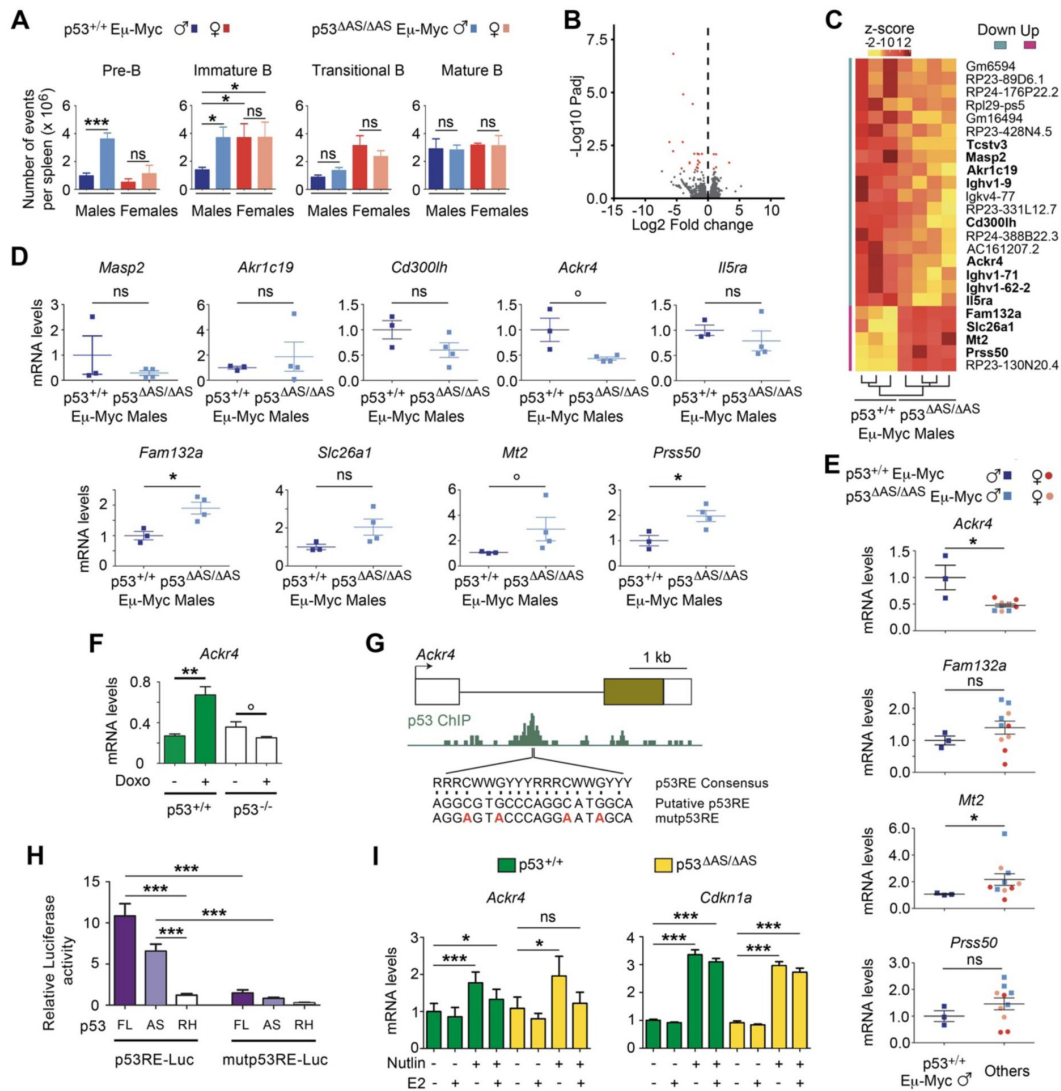


**Figure 3.**

### The loss of p53-AS isoforms affects *Acr4* expression in E $\mu$ -Myc male mice.

(A) B-cell subpopulations in spleens of 6 weeks-old  $p53^{+/+}$  E $\mu$ -Myc and  $p53^{\Delta AS/\Delta AS}$  E $\mu$ -Myc mice. Means  $\pm$  SEM (n=6 per genotype). (B-C) RNAseq analysis of spleens from  $p53^{+/+}$  E $\mu$ -Myc (n=3) and  $p53^{\Delta AS/\Delta AS}$  E $\mu$ -Myc (n=4) 4-6 weeks-old male mice. Volcano plot (B), with differentially expressed genes (DEGs) in red. Unsupervised clustering heat-map plot (C), with DEGs ranked according to mean fold changes, and protein-coding genes in bold. (D) RT-qPCR analysis of candidate DEGs from spleens of  $p53^{+/+}$  E $\mu$ -Myc males and  $p53^{\Delta AS/\Delta AS}$  E $\mu$ -Myc males. Means  $\pm$  SEM (n=3-4 per genotype). (E) RT-qPCR analysis of indicated DEGs from spleens of 4-6 weeks-old  $p53^{+/+}$  E $\mu$ -Myc males,  $p53^{\Delta AS/\Delta AS}$  E $\mu$ -Myc males,  $p53^{+/+}$  E $\mu$ -Myc females and  $p53^{\Delta AS/\Delta AS}$  E $\mu$ -Myc females. Means  $\pm$  SEM (n=3-4 per sex and genotype). (F) *Acr4* is transactivated by p53 in response to stress. *Acr4* mRNAs in untreated or doxorubicin-treated WT and  $p53^{-/-}$  MEFs. Data from 2-3 MEFs per genotype (Younger et al., 2015). (G) A putative p53 response element in *Acr4* intron 1. Top: Map of the *Acr4* gene. (boxes: exons (brown box: translated region), black line: intron 1); middle: p53 ChIP in doxorubicin-treated MEFs according to ChIP-Atlas (SRX270554) (Oki et al., 2018); bottom: p53 Response Element (p53RE) consensus sequence (R=G or A, W=A or T, Y=C or T), the putative p53RE and its mutated counterpart. (H) Luciferase assays of the candidate p53RE. A 1.5 kb fragment containing the WT or mutant p53RE was cloned upstream a luciferase reporter, then transfected into  $p53^{-/-}$  MEFs together with an expression plasmid for full length p53 (FL), p53-AS or the DNA-binding mutant p53<sup>R270H</sup> (RH). Means  $\pm$  SEM (n=4-6). (I) In MEFs, p53 activation leads to an increased *Acr4* expression attenuated by estradiol. *Acr4* and *Cdkn1a* mRNAs were quantified by RT-qPCR from  $p53^{+/+}$  and  $p53^{\Delta AS/\Delta AS}$  MEFs, untreated or treated with 10  $\mu$ M Nutlin and/or 5  $\mu$ g/ml 17- $\beta$  estradiol (E2). Means  $\pm$  SEM from 4 independent experiments. In A, D, E, F, H, I \*\*\*P<0.001, \*\*P<0.01, \*P<0.05, °P<0.057, ns: non-significant in Student's t or Mann-Whitney tests.



abrogated, *Ackr4* transactivation (**Figure 3I**). By contrast, *Cdkn1a* was efficiently transactivated under both conditions in mutant and WT cells (**Figure 3I**). These data indicate that *Ackr4* is a p53 target gene whose p53-mediated transactivation can be inhibited by estrogens.

The *Mt2* gene, encoding the potentially oncogenic metallothionein-2 (Si and Lang, 2018), was less expressed in p53<sup>+/+</sup> Eμ-Myc male pre-tumoral splenocytes, which raised the possibility of its direct or indirect repression by p53, potentially through the binding of p53 or the DREAM complex at its promoter (Engeland, 2018; Peugeot and Selivanova, 2021). However, ChIP-Atlas reported no binding of these proteins at the *Mt2* promoter. Alternatively, evidence that Myc may impact on *Mt2* expression was obtained previously (Qin et al., 2021), and ChIP-Atlas reported Myc binding at the *Mt2* promoter in primary B-cells from lymph nodes of Eμ-Myc mice as well as Eμ-Myc-induced lymphoma cells (Figure S3D). This may suggest that the lower expression of *Mt2* in pre-tumoral splenic cells from p53<sup>+/+</sup> Eμ-Myc males (**Figure 3E**) might result from a subtle difference in Myc signalling.

## Relevance of *ACKR4* expression in Burkitt lymphomas

Murine and human alternatively spliced p53 isoforms exhibit structural differences (Marcel et al., 2011) and the ChIP-Atlas database (Oki et al., 2018) does not report p53 binding to the human *ACKR4* intron 1. Nevertheless, we found that p53 activation in human cells also led to an increased *ACKR4* expression abrogated by 17-β estradiol, whereas 17-β estradiol had no significant effect on the p53-mediated transactivation of *CDKN1A* (**Figure 4A**). This led us to investigate the potential relevance of *ACKR4* expression in human B-cell lymphomas. We analyzed public databases of B-cell lymphoma patients with clinical and gene expression information. We first analyzed #GSE4475 (Hummel et al., 2006), a dataset of mature aggressive B-cell lymphomas previously used to define Burkitt lymphoma-like specific transcriptomes, comprising 159 patients (91 men, 68 women) with clinical follow-up. Overall, *ACKR4* gene expression was not significantly different between male and female patients (**Figure 4B**, left). However, average mRNA levels appeared higher in males when we considered the 30% patients of each sex with the highest *ACKR4* expression (**Figure 4B**, right). Strikingly, when we compared the survival of 30% patients with the highest *ACKR4* mRNA levels to the survival of the 30% patients with the lowest *ACKR4* mRNA levels, high *ACKR4* expression correlated with a better prognosis in men, but not in women (**Figure 4C**). By contrast, for *MT2A*, the human homolog of *Mt2*, differences in mRNA levels did not correlate with significant differences in survival for either sex (Figure S4A).

We also analyzed dataset #GSE181063 (Lacy et al., 2020), comprising mostly diffuse large B-cell lymphomas (DLBCL; 613 men, 536 women) and a few Burkitt lymphomas (65 men, 18 women). We found no difference in survival curves of DLBCL patients with low versus high *ACKR4* levels, neither in men nor in women. However, there was again an increased survival for Burkitt lymphoma male patients with high *ACKR4* expression, but not for women (Figure S4B). Finally, we analyzed #phs000235 (Morin et al., 2011), a Burkitt lymphoma-specific dataset (65 men, 37 women) comprising mostly patients diagnosed at 0-17 years of age, hence providing cohorts homogeneous for both tumor type and age of onset. Again, *ACKR4* was expressed at higher levels in a subset of male patients (**Figure 4D**) and high *ACKR4* expression correlated with a better prognosis only in males (**Figure 4E**). We thus conclude that, as in Eμ-Myc mice, *ACKR4* is a male-specific positive prognostic factor in Burkitt lymphoma, the archetype of MYC-driven B-cell lymphomas.

## Discussion

In this report we analyzed a mouse model with a specific deletion of the alternatively spliced (AS) exon of the *Trp53* gene. Despite a subtle phenotype, this model revealed that a male-specific protective effect against Eμ-Myc-induced B-cell lymphomas is lost in the absence of p53-AS

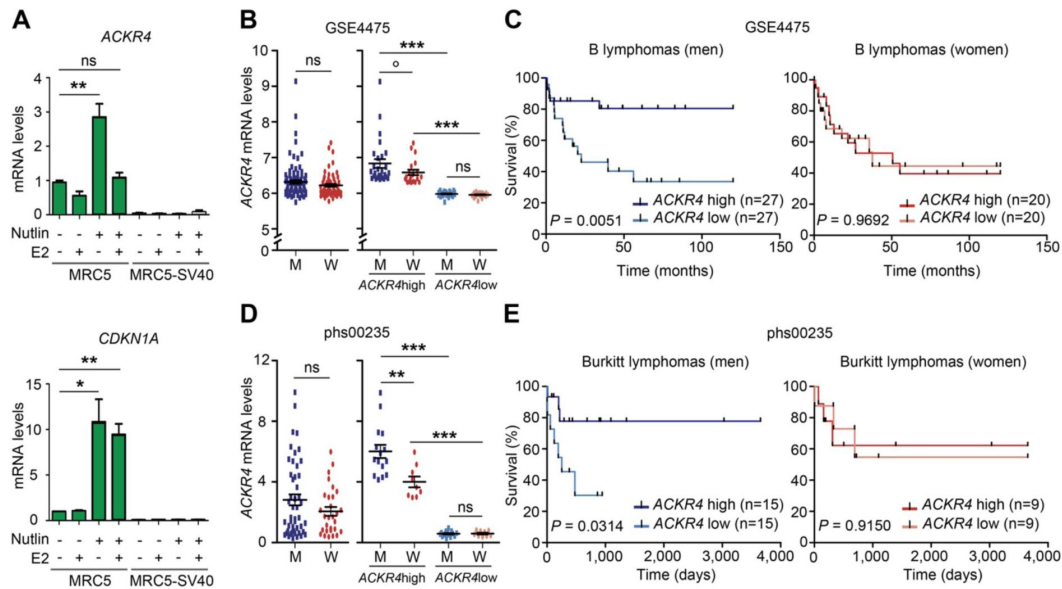


**Figure 4.**

***ACKR4* is a male-specific prognostic factor in Burkitt lymphoma.**

(A) In human cells, p53 activation leads to an increased *ACKR4* expression abrogated by estradiol. *ACKR4* and *CDKN1A* mRNAs were quantified by RT-qPCR from p53-proficient (MRC5) and p53-deficient (MRC5-SV40) human fibroblasts, untreated or treated with Nutlin and/or estradiol (E2). Means  $\pm$  SEM from 4 independent experiments. (B-C) Analysis of lymphoma dataset #GSE4475. *ACKR4* gene expression was plotted for all lymphoma patients with clinical follow-up (91 men [M], 68 women [W]), classified according to sex (B, left). Gene expression (B, right) or survival curves (C) were plotted for the 30% patients (27 men, 20 women) with the highest or lowest *ACKR4* expression, classified according to sex. (D-E) Analysis of Burkitt lymphoma-specific dataset #phs00235. *ACKR4* gene expression was plotted for all patients with a Burkitt lymphoma diagnosed at age 0-17 (48 males, 29 females), classified according to sex (D, left). Gene expression (D, right) or survival curves (E) were plotted for the 30% patients (15 men, 9 women) with the highest or lowest *ACKR4* expression, classified according to sex. Statistical analyses by Student's *t* or Mann-Whitney tests (A, B, D) and Mantel-Cox (C, E) test. \*\*\* $P < 0.001$ , \*\* $P < 0.01$ , \* $P < 0.05$ , ° $P = 0.054$ , ns: non-significant.

isoforms.  $p53^{\Delta AS/\Delta AS}$  males also appeared more prone to develop spontaneous lymphomas, suggesting that the sex-specific protective effect conferred by p53-AS isoforms might not be restricted to the E $\mu$ -Myc model.

Our transcriptomic data from splenocytes of  $p53^{+/+}$  E $\mu$ -Myc and  $p53^{\Delta AS/\Delta AS}$  E $\mu$ -Myc males disclosed very few differentially expressed genes, and highlighted *Ackr4* as a male-specific positive prognostic factor in E $\mu$ -Myc-induced lymphomas. Mechanistically, we identified *Ackr4*, expressed at low levels in splenocytes, as a p53 target gene that may be transactivated by p53- $\alpha$  and/or p53-AS according to luciferase assays. Because the loss of p53-AS isoforms correlated with an apparent decrease in p53- $\alpha$  levels in both thymocytes and tumor lymph nodes, the decreased transactivation of *Ackr4* in splenocytes of  $p53^{\Delta AS/\Delta AS}$  E $\mu$ -Myc males might result from the loss of p53-AS isoforms *per se*, but also possibly from a decrease in p53- $\alpha$  levels. Furthermore, we observed that 17- $\beta$  estradiol can inhibit the p53-mediated transactivation of *Ackr4*. Together, our data suggest that *Ackr4* may be regulated by p53- $\alpha$ , p53-AS and estrogens, likely accounting for sex-specific and p53-status dependent differences in gene expression.

Our analyses reveal that in both mice and humans, *Ackr4/ACKR4* is a male-specific prognostic factor in Burkitt-like lymphomas. In fact, *Ackr4* most likely acts as a tumor suppressor of Myc-driven B-cell lymphomas because: 1) in lymph nodes, *Ackr4* creates a gradient of the chemokine Ccl21, a ligand of the chemokine receptor Ccr7 (Bastow et al., 2021 [↗](#); Ulvmar et al., 2014 [↗](#)); 2) the *Ackr4*-mediated sequestration of Ccl21 impairs the Ccr7 signalling cascade, which may lead to decreased Myc activity (Shi et al., 2015 [↗](#)); 3) Ccr7 is also required for lymphoma cell lodging to secondary lymphoid organs, and Ccr7 deficiency was shown to delay E $\mu$ -Myc-induced lymphomagenesis (Rehm et al., 2011 [↗](#)). Thus, in  $p53^{+/+}$  E $\mu$ -Myc male pre-tumoral splenocytes, an increased *Ackr4* expression might delay lymphomagenesis in part by attenuating Myc signalling. Indeed, the observed lower expression of *Mt2*, known to be regulated by Myc (Qin et al., 2021 [↗](#)), appears consistent with this hypothesis. Importantly, *Ackr4* was previously found to inhibit the growth and metastasis of breast, cervical, colorectal, hepatocellular and nasopharyngeal cancer cells (Feng et al., 2009 [↗](#); Hou et al., 2013 [↗](#); Ju et al., 2019 [↗](#); Shi et al., 2015 [↗](#); Zhu et al., 2014 [↗](#)), although no report mentioned any sex-specific bias for cancers occurring in both sexes. Our data provide evidence that sex-specific differences in *Ackr4* expression may have prognostic value. This suggests that measuring *ACKR4* gene expression in male patients with Burkitt lymphoma could be useful to identify the patients at higher risk, for whom specific therapeutic regimens might be required.

Interestingly, our data suggested that *Mt2* might be a male-specific negative prognostic factor in murine E $\mu$ -Myc induced lymphomas, but *MT2A* expression levels had no prognostic value in human lymphomas. A possible explanation for this discrepancy is suggested by the fact that *Mt2* is regulated by Myc. A translocation leading to MYC overexpression drives oncogenesis in all Burkitt lymphomas, but half of them exhibit additional missense MYC mutations enhancing its tumorigenicity (Chakraborty et al., 2015 [↗](#)). The transcriptional program of a WT and two lymphoma-associated Myc mutants were recently compared, and we noticed that one of the mutants led to an alteration in *Mt2* expression (Mahani et al., 2021 [↗](#)), which would abrogate any potential prognostic value.

Finally, a polymorphism in the *MDM2* gene promoter provided evidence that sex-specific hormones may affect p53 signalling and tumorigenesis (Bond and Levine, 2007 [↗](#)). More recently, a higher frequency of *TP53* mutations in men, together with an increased vulnerability to alterations of X-linked genes encoding p53 regulators, were proposed to explain a higher cancer incidence and death in male patients (Haupt et al., 2019 [↗](#)). Here, on the contrary, male mice and a subset of male patients were more efficiently protected against Burkitt-like lymphomas, which adds another layer of complexity to sex-specific differences in tumorigenesis. The p53 pathway thus underlies cancer sex-disparities through multiple mechanisms, that may notably include variations in p53 isoforms or *Ackr4* expression.

## Materials and Methods

### Mice

Design and construction of the p53<sup>ΔAS</sup> mouse model was previously described (Simeonova et al., 2013 [↗](#)). A minimum of 10 backcrosses with C57Bl6/J mice of both sexes (Charles River Laboratories) were performed before establishing the cohorts of p53<sup>+/+</sup> and p53<sup>ΔAS/ΔAS</sup> littermate mice used in this study. Mouse genotyping with multiple primer sets confirmed >99% C57Bl6/J genetic background after 10 backcrosses (primer sequences available upon request). Cohorts of p53<sup>+/+</sup> Eμ-Myc and p53<sup>ΔAS/ΔAS</sup> Eμ-Myc mice were established with identical parental origin of the Eμ-Myc transgene. For all experiments, mice housing and treatment were conducted according to Institutional Animal Care and Use Committee of the Institut Curie.

### Cells and cell culture reagents

Mouse embryonic fibroblasts (MEFs) were isolated from 13.5 days post-coitum embryos and cultured in a 5% CO<sub>2</sub> and 3% O<sub>2</sub> incubator, in DMEM Glutamax (GIBCO), with 15% FBS (PAN Biotech), 100 μM 2-mercaptoethanol (Millipore), 0.1 mM Non-Essential Amino-Acids and Penicillin/Streptomycin (GIBCO) for less than 5 passages, except for 3T3 experiments, performed in a 5% CO<sub>2</sub> incubator for 9 passages. Cells were treated for 24h with 0.5 μg/ml Doxorubicin (Sigma-Aldrich), 15 μM Etoposide (Sigma-Aldrich), 10 μM Nutlin 3a (Vassilev et al., 2004 [↗](#)) (Sigma-Aldrich) and/or 5 μg/ml 17β-Estradiol (Merck). At least 3 independent experiments with at least 2 independent littermate MEF clones of each genotype and each sex were performed to measure DNA damage responses. For estradiol assays, four independent experiments with three independent MEF male clones of each genotype were performed. Human lung fibroblast MRC5 and its SV40-transformed derivatives were cultured in a 5% CO<sub>2</sub> and 3% O<sub>2</sub>-regulated incubator in MEM medium without Phenol Red (Gibco), completed with 10% FBS, 2 mM L-glutamine (Gibco), 1 mM pyruvate, 0.1 mM Non-Essential Amino-Acids, and penicillin/streptomycin, and treated for 24h with 10 μM Nutlin 3a (Sigma-Aldrich) and/or 5 μg/ml 17β-Estradiol (Merck). Four independent experiments were performed.

### Quantitative RT-PCR

Total RNAs were extracted using nucleospin RNA II (Macherey-Nagel), reverse-transcribed using superscript IV (Invitrogen), and real-time quantitative PCRs were performed on an ABI PRISM 7500 using Power SYBR Green (Applied Biosystems) as previously described (Simeonova et al., 2012 [↗](#)). For quantification of p53 isoforms in healthy tissues, a forward primer in exon 10 and a reverse primer encompassing the boundary between exons 10 and 11 were used for p53-α amplification, whereas the same forward primer and a reverse primer located in exon AS were used for p53-AS amplification (see Table S2 for primer sequences). To determine the AS/α mRNA ratios, expression levels were compared with a standard curve generated by serial dilutions of a plasmid containing both p53-AS and p53-α cDNAs.

### Western blots

Thymocytes were lysed in RIPA buffer (50 mM Tris-HCl pH 8, 150 mM NaCl, 5 mM EDTA, 0.5% deoxycholic acid, 0.1% SDS, 1% NP-40) with a cocktail of protease inhibitors (Roche) and 1 mM PMSF (Sigma). Whole-cell extracts were sonicated three times for 10 s and centrifuged at 13 000 r.p.m. for 30 min to remove cell debris. MEFs or B-cell lymphomas were lysed in Giordano's buffer (50 mM Tris-HCl pH 7.4, 250 mM NaCl, 5 mM EDTA, 0.1% Triton X-100) with a cocktail of protease inhibitors (Roche) and 1 mM PMSF (Sigma). Protein lysate concentration was determined by BCA assay (Thermo Scientific) and 30 μg of each lysate was fractionated by SDS-PAGE on a 4-12% polyacrylamide gel and transferred onto PDVF membrane (Amersham). Membranes were

incubated with antibodies against p53 (CM5, Novocastra), myc (9E-10, Santa Cruz), p21 (F-5, Santa Cruz) and actin (actin-HRP sc47778, Santa Cruz) and revealed with SuperSignal West femto detection reagent (Thermo Scientific).

## Apoptosis Assays

Six weeks-old p53<sup>+/+</sup> and p53<sup>ΔAS/ΔAS</sup> male mice were whole-body irradiated with 5 Gy of  $\psi$ -irradiation. Mice were sacrificed 4h later and thymocytes were recovered, stained with AnnexinV-FITC Apoptosis detection kit (Abcam), then analyzed by flow cytometry using FlowJo.

## Cell-Cycle assays

Log phase MEFs were irradiated at room temperature with a CS  $\psi$ -irradiator at doses of 3 or 10 Gy, incubated for 24 h, then pulse-labeled for 1h with 10  $\mu$ M BrdU, fixed in 70% ethanol, double-stained with FITC anti BrdU and propidium iodide, and sorted by flow cytometry using a BD FACSort. Data were analyzed using FlowJo.

## Oncogene-induced tumor xenografts

MEFs with the indicated genotypes were sequentially infected with pWZL-E1A12S and pBABE-Hrasv12 viruses as previously described (Toledo et al., 2006 [↗](#)). In total,  $5 \times 10^6$  E1A- and Ras-(E1A+Ras) expressing MEFs of each genotype were injected subcutaneously into the flanks of 7-weeks-old female athymic nude mice (at least 4 mice per genotype) and tumor volumes were determined 1, 8, 15, 21 and 25 days after injection. Importantly, populations of (E1A+Ras)-expressing cells were used to minimize potential differences in expression levels that could result from independent viral insertion sites.

## Cell sorting of B-cell sub-populations

Splenocytes were recovered from 6 weeks-old asymptomatic mice and incubated with DAPI and the following antibodies: APC rat anti-mouse CD45R/B220, FITC rat anti-mouse CD43, PE rat anti-mouse IgM and BV605 rat anti-mouse IgD (BD Pharmingen). First, the B220+CD43-cells were selected by flow cytometry from DAPI negative living cells, yielding subsequently 4 different B subpopulations based on IgM and IgD labeling: IgM-/IgD-preB lymphocytes, IgM low/IgD-immature B lymphocytes, IgM high/IgD-transitional B lymphocytes and IgM+/IgD+ mature B lymphocytes.

## RNA-Seq analysis

Total RNA was extracted from the spleen of 4-6 weeks-old asymptomatic mice using nucleospin RNA II (Macherey-Nagel). The quality of RNA was checked with Bioanalyzer Agilent 2100 and RNAs with a RIN (RNA integrity number)  $\geq 6$  were retained for further analysis. RNA was depleted from ribosomal RNA, then converted into cDNA libraries using a TruSeq Stranded Total Library preparation kit (Illumina). Paired-end sequencing was performed on an Illumina MiSeq platform. Reads were mapped to the mouse genome version GRCm38 and counted on gene annotation gencode.vM18 with featureCounts (Liao et al., 2014 [↗](#)). Differentially expressed genes of C57Bl6/J genetic background with an adjusted p-value  $< 0.05$  were identified using the DESeq2 R package (Love et al., 2014 [↗](#)).

## Luciferase assays

The candidate p53 responsive element (p53 RE) in the *Ackr4* promoter was identified by using the JASPAR database of binding profiles (Fornes et al., 2020 [↗](#)) with the position weight matrix scanner PWMscan (Ambrosini et al., 2018 [↗](#)). A 1.5 kb fragment from *Ackr4* intron 1, containing a WT or mutant p53 RE at its center, was cloned upstream a SV40 minimal promoter and a luciferase reporter gene in the backbone of a PGL3 plasmid (Promega). We used lipofectamine 2000 to transfect p53<sup>-/-</sup> MEFs with 2  $\mu$ g of either luciferase expression vector, 2  $\mu$ g of an expression vector for p53<sup>WT</sup>, p53<sup>AS</sup> or the DNA-binding mutant p53<sup>R270H</sup>, and 30 ng of a renilla luciferase

expression plasmid (pGL4.73, Promega) for normalization. Transfected cells were incubated for 24 h then trypsinized, resuspended in 75  $\mu$ l culture medium with 7.5% FBS and transferred into a well of an optical 96-well plate (Nunc). The dual-glo luciferase assay system (Promega) was used according to the manufacturer's protocol to lyse the cells and read firefly and renilla luciferase signals. Results were normalized, then the average luciferase activity in cells transfected with the WT p53RE luciferase reporter and the p53<sup>R270H</sup> expression plasmid were assigned a value of 1.

## Statistical Analyses

Student's unpaired *t* tests were used in most Figures to analyze differences between WT vs  $\Delta$ AS values. Log-Rank Mantel-Cox were used to analyze Kaplan-Meier tumor-free survival curves. Analyses were performed using Graphpad Prism 5, and values of  $p < 0.05$  were considered significant.

## Data availability

RNA sequencing data have been deposited in the Gene Expression Omnibus (GEO) under the accession code GSE209708.

## Acknowledgements

This project was supported by grants from the Comité Tumeurs of Fondation de France (to F.T.), the Comité Ile-de-France and Comité national (Labellisation 2014-18) of the Ligue Nationale Contre le Cancer (to F.T.), and the Fondation ARC pour la recherche sur le Cancer (to F.T.). I.S., E.E. and J.R. were PhD fellows of the Ministère de la Recherche; J.L. and A.M. were post-doctoral fellows of Cancéropôle Ile-de-France and Institut National du Cancer. M.G. was paid by European Research Council 875532-Prostator-ERC-2019-PoC attributed to A.M.; J.C.B. was supported by Cancer Research-UK. We thank K. Fernandes for his participation in making the  $\Delta$ AS mutation, and members of the Institut Curie platforms: I. Grandjean, H. Gautier, C. Daviaud, M. Garcia, M. Verlhac, A. Fosse and P. Bureau (animal facility); S. Baulande and S. Lameiras (NGS); M. Huerre, A. Nicolas and R. Leclere (histopathology); Z. Maciorowski, A. Viguier and S. Grondin (flow cytometry).

## Author Contributions

F.T, J.C.B. and I.S. initiated the project; F.T., B.B. and A.F. designed the research and analyzed data; B.B., A.F., I.S., J.L., A.M., V.L., F.T., A.H., W.V.-Z., E.E. and J.R. performed the research; M.G., M.P. and A.M. analyzed RNAseq data; F.T. acquired funding; F.T., A.F. and B.B. wrote the paper.

## Declaration of interests

The authors declare no competing interest.

## Supplemental Information



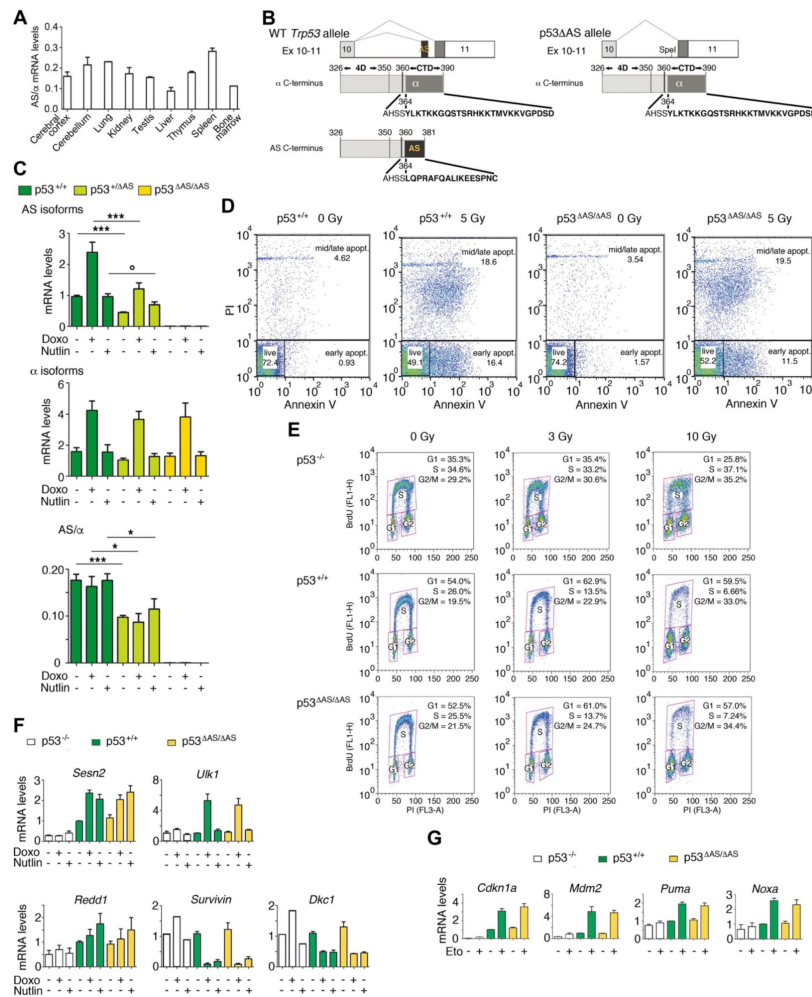


**Figure S1.**

### Description of the p53 $\Delta$ AS mouse model and analysis of p53 $\Delta$ AS/ $\Delta$ AS thymocytes and fibroblasts.

(A) Relative expression of p53 isoforms with an  $\alpha$  or AS C-terminus in tissues of wild-type mice. RNAs were prepared from the indicated tissues of wild-type mice, then p53-AS and p53- $\alpha$  mRNAs were quantified by RT-qPCR. Results are expressed as mean AS/a ratios  $\pm$  SD, from 3 independent experiments. (B) Comparative maps of the wild-type (WT) and  $\Delta$ AS *Trp53* alleles. Left, top: the 3' end of the WT *Trp53* gene is shown - black line: intron 10; boxes are for exons, with greytones for translated regions from exon 10 (light gray), exon 11 (dark gray), and exon AS (black). Left, below: the WT *Trp53* allele encodes proteins with two different C-termini. (4D: tetramerization domain, CTD: C-terminal domain). Right, top: the 3' end of the  $\Delta$ AS *Trp53* allele is shown; the AS exon was deleted and replaced by a SpeI restriction site. Right, below: the  $\Delta$ AS *Trp53* allele only enables the synthesis of proteins with the 'canonical'  $\alpha$  C-terminus. (C) Quantifications of p53 isoforms with an AS or an  $\alpha$  C-terminus, in mouse embryonic fibroblasts (MEFs) of the indicated genotypes, that were either untreated, or treated for 24hr with 0.5  $\mu$ g/ml doxorubicin (Doxo) or 10  $\mu$ M Nutlin. Means  $\pm$  SEM from  $>3$  experiments with  $\geq 2$  independent MEF clones of each genotype are shown. \*\*\* $P < 0.001$ , \* $P < 0.05$ ,  $^{\circ}P = 0.07$  by Student's t-test. (D) Apoptotic responses of p53<sup>+/+</sup> and p53<sup>AS/AS</sup> thymocytes. p53<sup>+/+</sup> and p53<sup>AS/AS</sup> mice were irradiated and their thymocytes were recovered and analyzed by FACS after annexin V-FITC staining. A typical experiment for cells of each genotype and condition is shown. Numbers indicate % cells, apopt.: apoptotic cells. (E) Cell cycle control of p53<sup>-/-</sup>, p53<sup>+/+</sup> and p53<sup>AS/AS</sup> fibroblasts. Asynchronous MEFs were exposed to 0-10 Gy  $\psi$ -irradiation, then after 24 hr cells were labelled with BrdU for 1 hr and analyzed by FACS. A typical experiment for cells of each genotype and condition is shown, with % of cells in G1, S and G2/M mentioned in each panel. (F) mRNA levels of the indicated genes were quantified in MEFs of the indicated genotypes left untreated or treated for 24 hr with 0.5  $\mu$ g/ml Doxorubicin (Doxo), 10  $\mu$ M Nutlin-3 (Nutlin). Means  $\pm$  SEM from at least 3 experiments with 2 independent MEF clones of p53<sup>+/+</sup> and p53<sup>AS/AS</sup> genotypes are shown. (G) mRNA levels of the indicated genes were quantified in MEFs of the indicated genotypes left untreated or treated for 24 hr with 15  $\mu$ M etoposide (Eto). Means  $\pm$  SEM from at least 3 experiments with 2 independent MEF clones per genotype.

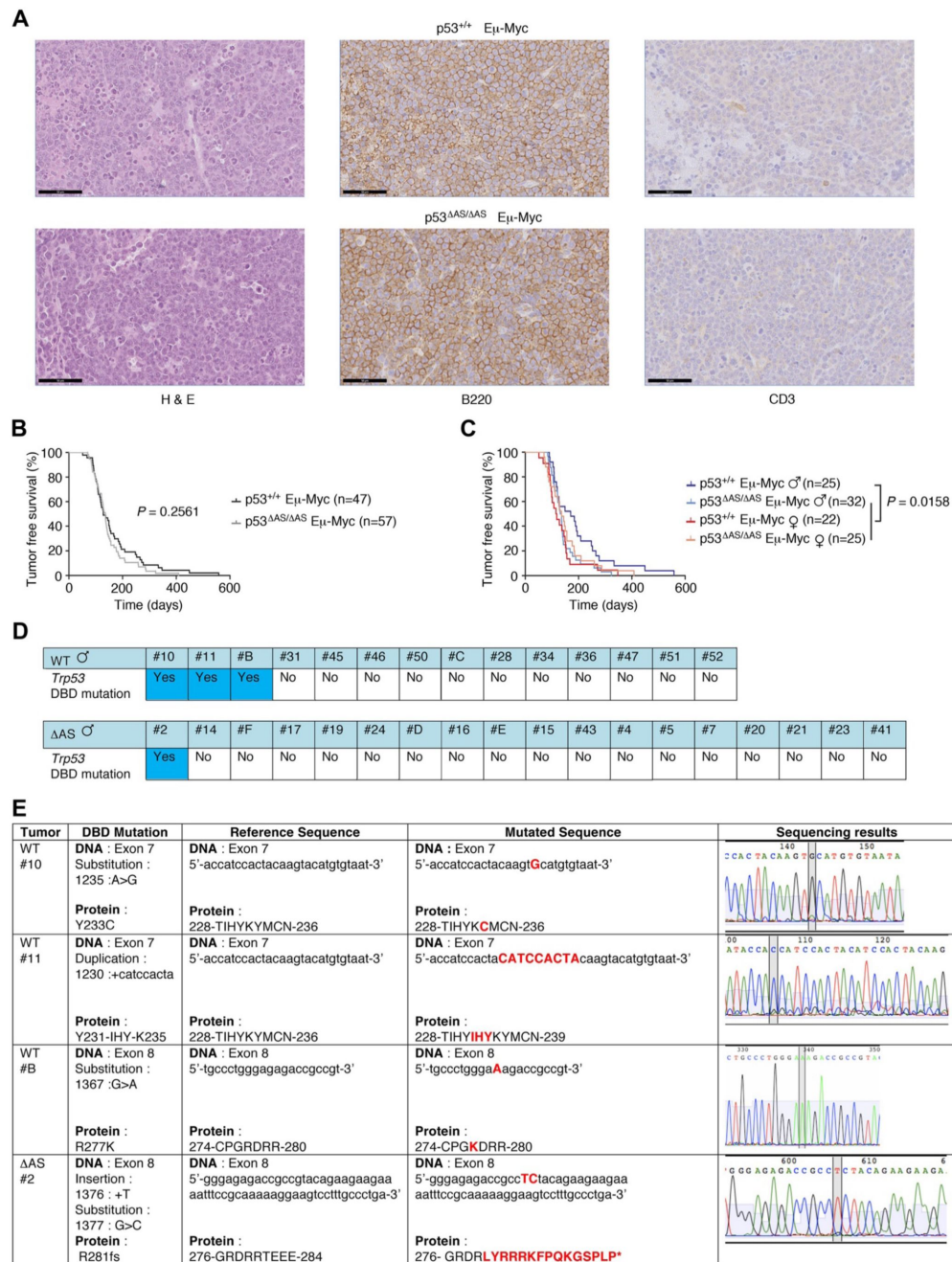


**Figure S2.**

### Analysis of tumors from $p53^{+/+}$ E $\mu$ -myc and $p53^{\Delta AS/\Delta AS}$ E $\mu$ -Myc mice.

(A) Histological analyses of E $\mu$ -Myc-induced tumor lymph nodes. Tumor lymph nodes were analyzed by Hematoxylin-Eosin staining (H & E), or antibodies against B220 (a B-cell specific marker) or CD3 (a T-cell specific marker).  $p53^{+/+}$  E $\mu$ -Myc and  $p53^{\Delta AS/\Delta AS}$  E $\mu$ -Myc mice developed similar B-cell lymphomas, characterized by massive tissue homogenization of the lymph node by B-cells. Scale bars=50  $\mu$ m. (B) Tumor-free survival of  $p53^{+/+}$  E $\mu$ -myc and  $p53^{\Delta AS/\Delta AS}$  E $\mu$ -Myc mice are similar when sexes are not considered ( $n$ =cohort size). (C) Increased tumor-free survival of  $p53^{+/+}$  E $\mu$ -myc males compared to  $p53^{\Delta AS/\Delta AS}$  E $\mu$ -Myc males,  $p53^{+/+}$  E $\mu$ -Myc females and  $p53^{\Delta AS/\Delta AS}$  E $\mu$ -Myc females ( $n$ =cohort size). Statistical analysis with Mantel-Cox test. (D) *Trp53* DNA sequencing of  $p53^{+/+}$  E $\mu$ -myc and  $p53^{\Delta AS/\Delta AS}$  E $\mu$ -Myc tumors. The portion of the *Trp53* gene encoding the DNA Binding domain (DBD), most frequently mutated in cancers, was sequenced for 14 tumors from  $p53^{+/+}$  (WT) E $\mu$ -myc males and 18 tumors from  $p53^{\Delta AS/\Delta AS}$  ( $\Delta AS$ ) E $\mu$ -myc males, and *Trp53* mutations were found in 3/14 and 1/18 tumors, respectively. (E) Details on the 4 *p53* mutations identified in (D).

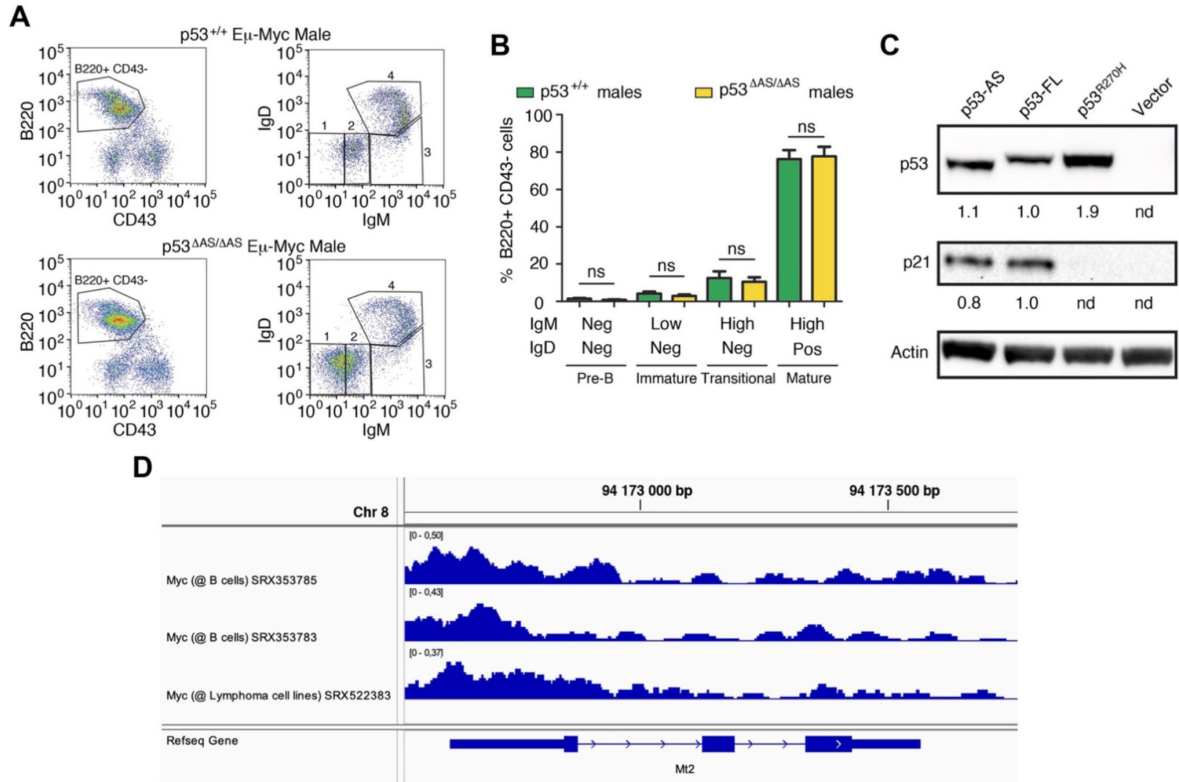


**Figure S3.**

### Analysis of pre-tumoral spleens.

(A) Cell sorting of B-cell subpopulations by FACS. Splenocytes were incubated with DAPI and the following antibodies: APC rat anti-mouse CD45R/B220, FITC rat anti-mouse CD43, PE rat anti-mouse IgM and BV605 rat anti-mouse IgD. First, the B220+CD43<sup>-</sup> cells were selected from DAPI negative living cells, subsequently yielding 4 different B subpopulations based on IgM and IgD labeling: IgM<sup>-</sup>/IgD<sup>-</sup> pre-B cells (box 1), IgM low/IgD<sup>-</sup> immature B cells (box 2), IgM high/IgD<sup>-</sup> transitional B cells (box 3) and IgM<sup>+</sup>/IgD<sup>+</sup> mature B cells (box 4). Typical results with a p53<sup>+/+</sup> Eμ-Myc male mouse and a p53<sup>ΔAS/ΔAS</sup> Eμ-Myc male mouse are shown. (B) The loss of p53-AS isoforms does not impair B-cell differentiation in 6 weeks-old non-transgenic male mice. Means ± SEM from 4 mice per genotype. ns: non-significant by Student's t-test. (C) Control for expression of p53-FL, p53-AS and p53<sup>R270H</sup> in luciferase assays. As a control to luciferase experiments reported in **Fig. 3H**, protein extracts from p53<sup>-/-</sup> MEFs transfected with expression plasmids for p53-FL, p53-AS or p53<sup>R270H</sup> were immunoblotted with antibodies against p53, p21 and actin. Quantifications are relative to actin. p53-FL and p53-AS were expressed at similar levels and both transactivated p21, whereas the DNA-binding mutant p53<sup>R270H</sup> was expressed at higher amounts but failed to transactivate p21, as expected. nd: not determined. (D) Evidence for Myc binding at the *Mt2* promoter in B-cells. ChIP-Atlas reports Myc binding to *Mt2* promoter sequences in primary B-cells from the lymph nodes of Eμ-Myc mice (SRX353785, SRX353783) and in Eμ-Myc-induced lymphoma cells (SRX522383). Chr: chromosome.

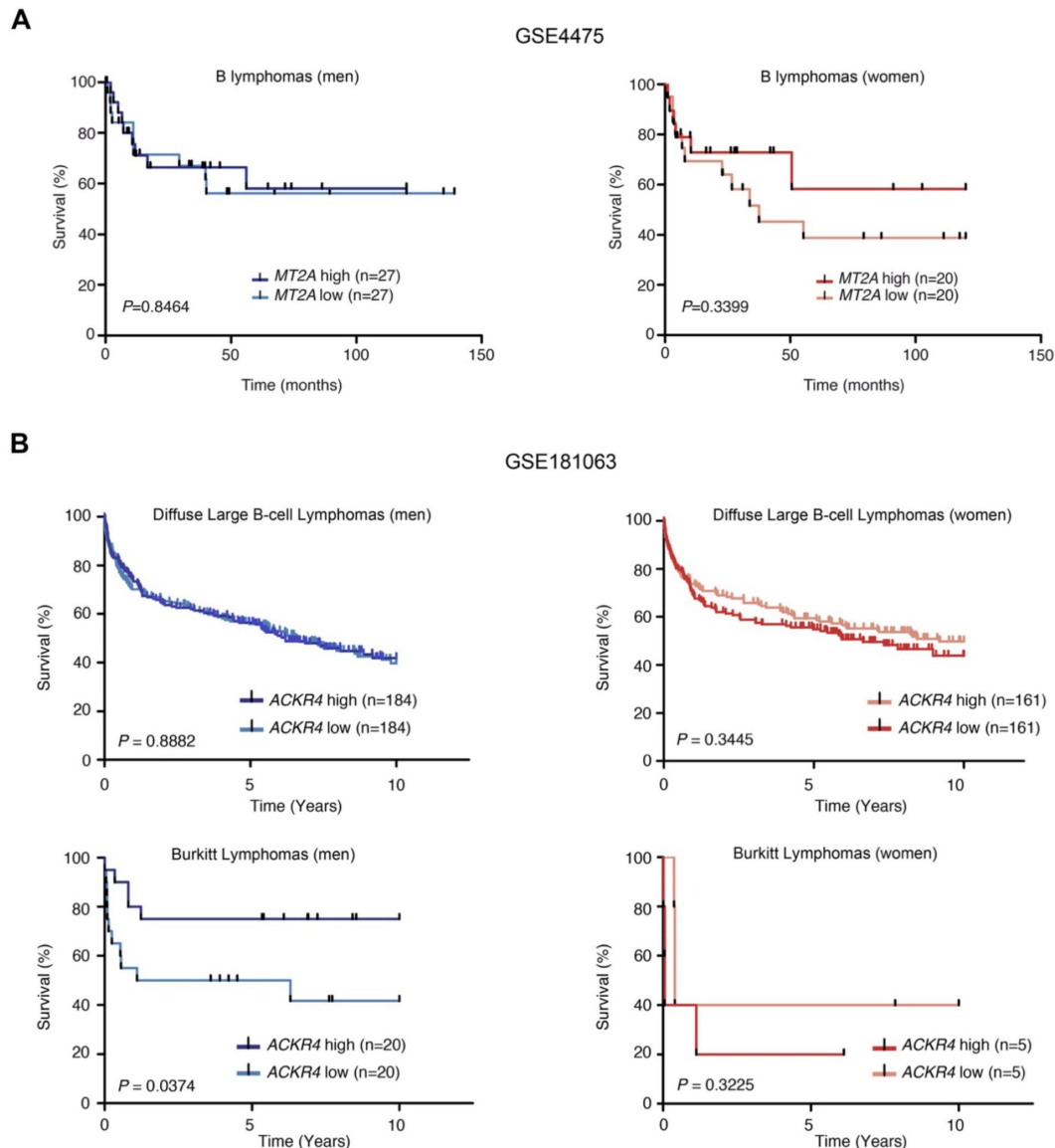


**Figure S4.**

**Further analyses of human B-cell lymphoma datasets.**

(A) *MT2A* gene expression is not a prognostic marker in human B-cell lymphomas. Survival curves for the 30% patients with the highest *MT2A* mRNA levels and the 30% patients with the lowest *MT2A* mRNA levels according to sex ( $n$ =cohort sizes), for patients from dataset #GSE4475. Statistical analyses by Mantel-Cox tests. (B) *ACKR4* is a prognostic factor in Burkitt lymphomas but not in diffuse large B-cell lymphomas. Survival curves of patients from dataset #GSE181063, for the 30% patients with the highest *ACKR4* mRNA levels and the 30% patients with the lowest *ACKR4* mRNA levels, classified according to sex ( $n$ =cohort sizes), and diagnosed with either a diffuse large B-cell (top) or a Burkitt (bottom) lymphoma. Statistical analyses by Mantel-Cox tests.

Gene	WT_Myc_1	WT_Myc_2	WT_Myc_3	$\Delta$ AS_Myc_1	$\Delta$ AS_Myc_2	$\Delta$ AS_Myc_3	$\Delta$ AS_Myc_4
<i>Ackr4</i>	267.610698766789	187.913317967838	103.698438238889	80.2839670298248	58.3264519788058	44.2019721676723	58.626719832054
<i>Cdkn1a</i>	1172.3897279307	1179.72136964871	1227.565295909	1248.51861547663	1018.37985154995	800.288338193645	1079.90417930643
<i>Mdm2</i>	4419.00743604647	4820.24950903391	5133.53980290714	4756.31040570283	4240.33305885918	4132.88439767736	5521.46447378284

**Table S1.**

**Expression of *Ackr4*, *Cdkn1a* and *Mdm2* in  $p53^{+/+}$  E $\mu$ -Myc and  $p53^{\Delta AS/\Delta AS}$  E $\mu$ -Myc male splenocytes.**

Read numbers for the indicated genes, obtained by Bulk RNA-seq from the spleens of three  $p53^{+/+}$  E $\mu$ -Myc (WT\_Myc) and four  $p53^{\Delta AS/\Delta AS}$  E $\mu$ -Myc ( $\Delta$ AS\_Myc) male mice.

Locus	Species	Usage	Forward	Reverse
<i>Trp53</i>	Mouse	Genotyping	5' AAGGGGTATGAGGGACAAGG 3'	5' GAAGACAGAAAAGGGGAGGG 3'
<i>Eμ-Myc</i>	Mouse	Genotyping	5' ACCCAGGCTAAGAAGGCAAT 3'	5' CGTCACTCCCTCTGTCTCT 3'
<i>Trp53</i> exon4	Mouse	Sequencing	5' CAGAGCAGAAAAGGACTTGG 3'	5' GCTAAAAAGGTTCAAGGCAAA 3'
<i>Trp53</i> exon5-6	Mouse	Sequencing	5' TGGTGTCTGGACAATGTGTT 3'	5' TAGCACTCAGGAGGGTGAGG 3'
<i>Trp53</i> exon7-9	Mouse	Sequencing	5' TGCCGAACAGGTGGAATATC 3'	5' CCTTGGTACCTGAGGGTGA 3'
<i>Akr4</i>	Mouse	RT-qPCR	5' GCACCTCTCCAGCTTAAACA 3'	5' AATAGTATTCCGTGACTGGTTCAG 3'
<i>Akr1c19</i>	Mouse	RT-qPCR	5' AGTTGCCTACTGTGCTCTGGAT 3'	5' GAGAAGTGGAGAGCTGGGTCTA 3'
<i>Bax</i>	Mouse	RT-qPCR	5' CGGCGAATTGGAGATGAACT 3'	5' CCGTGTCCACGTCAGCAA 3'
<i>Cdkn1a</i>	Mouse	RT-qPCR	5' GCAGACCAGCTGACAGATTTC3'	5' TTCAGGGTTTTCTCTTCGAGAAG 3'
<i>Cd300lh</i>	Mouse	RT-qPCR	5' GAACATTGGCCAGGTGACTCA 3'	5' AAGAAGGAGATGCTGCTCAACAG 3'
<i>Fam132a</i>	Mouse	RT-qPCR	5' GACAAGAAGACTCTGGTGGAACTG 3'	5' AGGAAGGCGCCCTGAGTAGT 3'
<i>Fas</i>	Mouse	RT-qPCR	5' ATGCACACTCTGCGATGAAG 3'	5' CAGTGTCCACAGCCAGGAGA 3'
<i>Il5a</i>	Mouse	RT-qPCR	5' CCGCTGCTTCGTCITGTTA 3'	5' CAACCTGGTCCATAGATGACACA 3'
<i>Masp2</i>	Mouse	RT-qPCR	5' CCAATGAGAAGCCGTTCA 3'	5' GAGACACTCTGCATTATCCACAT 3'
<i>Mdm2</i>	Mouse	RT-qPCR	5' GTCTACCGAGGGTGCTGCAA 3'	5' AAGCAATGGTTTTGGTCTAACCA 3'
<i>Mt2</i>	Mouse	RT-qPCR	5' ACAATGCAAATGTACTTCCTGC 3'	5' CACTTCGCACAGCCACG 3'
<i>Myc</i>	Mouse	RT-qPCR	5' CCACCAGCAGCGACTCTGA 3'	5' TCCACAGACACCACATCAATTC 3'
<i>Noxa</i>	Mouse	RT-qPCR	5' CCTGGGAAGTCGAAAAGAG 3'	5' GAGCACACTCGTCTCAAGTCT 3'
<i>Prss50</i>	Mouse	RT-qPCR	5' CGTGGCCCAATTGCTTGA 3'	5' GCTCCCCGCCCTCACT 3'
<i>Puma</i>	Mouse	RT-qPCR	5' GAGCGCGGAGACAAGAA 3'	5' GAGTCCCATGAAGAGATTGTACATGA 3'
<i>Redd1</i>	Mouse	RT-qPCR	5' GAGTCCCTGGACAGCAGCAA 3'	5' CATCCAGGTATGAGGAGTCTCTCT 3'
<i>Sesn2</i>	Mouse	RT-qPCR	5' CTTCGCCCACTCAGAGAAGGT 3'	5' CTTGATGCGGGCTTCA 3'
<i>Slc26a1</i>	Mouse	RT-qPCR	5' GCCACTGCCCTTACTCTGATG 3'	5' GCCGGAGGATACCCATGAG 3'
<i>Survivin</i>	Mouse	RT-qPCR	5' TGTTTTTCTGCTTTAAGGAATTGG 3'	5' TCTATGCTCCTCTATCGGGTTGTC 3'
<i>Test3</i>	Mouse	RT-qPCR	5' CTCAGCTGTTGGAATAAGTTC 3'	5' CCATGGATCCCTGAAGGTAAATC 3'
<i>Trp53-α</i>	Mouse	RT-qPCR	5' AAAGGATGCCCATGCTACAGA 3'	5' TCTTGGTCTCAGGTAGCTGGAG 3'
<i>Trp53-ΔS</i>	Mouse	RT-qPCR	5' AAAGGATGCCCATGCTACAGA 3'	5' TGAAGTATGGGAGCTAGCAGTT 3'
<i>Ulk1</i>	Mouse	RT-qPCR	5' TGTACATGGCTCCTGAGGTCAT 3'	5' CTCACAGGTCAGCCTTCC 3'
<i>Ppia</i>	Mouse	RT-qPCR control (MEFs)	5' TCTCCTTCGAGCTGTTTGA 3'	5' CAGTGTCTCAGAGCTCGAAAAGTTT 3'
<i>Rplp0</i>	Mouse	RT-qPCR control (MEFs)	5' CGACTGGAAGTCCAACACTAC 3'	5' ATCTGTGCATCTGCTTG 3'
<i>Il2rg</i>	Mouse	RT-qPCR control (spleen)	5' GGAGTCCAAGTCTCATG 3'	5' TGTAGAAGTCAGGATCAAATCAGCTT 3'
<i>Polr2a</i>	Mouse	RT-qPCR control (spleen, thymus)	5' CTTTGAGAAACGGTGGATGTC 3'	5' TCCCTTCATCGGGTCACTCT 3'
<i>Vps4a</i>	Mouse	RT-qPCR control (thymus)	5' GACAACGTCAACCTCCAGAAA 3'	5' TCTGTGGCTTTTGTACCAGAT 3'
<i>ACKR4</i>	Human	RT-qPCR	5' ACTGCTCCTCTGCGGACTAC 3'	5' GCCATTCAITTCATTTCTCAT 3'
<i>CDKN1A</i>	Human	RT-qPCR	5' ACCATGTGGACCTGCTACTGCTT 3'	5' AGAAGATGATAGAGCGGGCCTTGA 3'
<i>PPIA</i>	Human	RT-qPCR control	5' CATCTGCACTGCCAAGACTGA 3'	5' TTCATGCTCTTTTCACTTTGC 3'
<i>RPLP0</i>	Human	RT-qPCR control	5' CTTGTCTGTGGAGCGATTACAC 3'	5' TCAGCCAAGAAGGCCTTGA 3'

Table S2.

Primer Sequences.



## References

1. Abascal F, Ezkurdia I, Rodriguez-Rivas J, Rodriguez JM, del Pozo A, Vázquez J, Valencia A, Tress ML (2015) **Alternatively Spliced Homologous Exons Have Ancient Origins and Are Highly Expressed at the Protein Level** *PLoS Comput Biol* **11** <https://doi.org/10.1371/journal.pcbi.1004325>
2. Adams JM, Harris AW, Pinkert CA, Corcoran LM, Alexander WS, Cory S, Palmiter RD, Brinster RL (1985) **The c-myc oncogene driven by immunoglobulin enhancers induces lymphoid malignancy in transgenic mice** *Nature* **318**:533–538 <https://doi.org/10.1038/318533a0>
3. Ambrosini G, Groux R, Bucher P (2018) **PWMScan: a fast tool for scanning entire genomes with a position-specific weight matrix** *Bioinformatics* **34**:2483–2484 <https://doi.org/10.1093/bioinformatics/bty127>
4. Anbarasan T, Bourdon J-C (2019) **The Emerging Landscape of p53 Isoforms in Physiology, Cancer and Degenerative Diseases** *Int J Mol Sci* **20** <https://doi.org/10.3390/ijms20246257>
5. Arai N, Nomura D, Yokota K, Wolf D, Brill E, Shohat O, Rotter V (1986) **Immunologically distinct p53 molecules generated by alternative splicing** *Mol Cell Biol* **6**:3232–3239 <https://doi.org/10.1128/mcb.6.9.3232-3239.1986>
6. Bastow CR *et al.* (2021) **Scavenging of soluble and immobilized CCL21 by ACKR4 regulates peripheral dendritic cell emigration** *Proc Natl Acad Sci U S A* **118** <https://doi.org/10.1073/pnas.2025763118>
7. Blencowe BJ (2017) **The Relationship between Alternative Splicing and Proteomic Complexity** *Trends Biochem Sci* **42**:407–408 <https://doi.org/10.1016/j.tibs.2017.04.001>
8. Bond GL, Levine AJ (2007) **A single nucleotide polymorphism in the p53 pathway interacts with gender, environmental stresses and tumor genetics to influence cancer in humans** *Oncogene* **26**:1317–1323 <https://doi.org/10.1038/sj.onc.1210199>
9. Bourdon J-C, Fernandes K, Murray-Zmijewski F, Liu G, Diot A, Xirodimas DP, Saville MK, Lane DP (2005) **p53 isoforms can regulate p53 transcriptional activity** *Genes Dev* **19**:2122–2137 <https://doi.org/10.1101/gad.1339905>
10. Brayton CF, Treuting PM, Ward JM (2012) **Pathobiology of Aging Mice and GEM: Background Strains and Experimental Design** *Vet Pathol* **49**:85–105 <https://doi.org/10.1177/0300985811430696>
11. Chakraborty AA, Scuoppo C, Dey S, Thomas LR, Lorey SL, Lowe SW, Tansey WP (2015) **A common functional consequence of tumor-derived mutations within c-MYC** *Oncogene* **34**:2406–2409 <https://doi.org/10.1038/onc.2014.186>
12. Chow MT, Luster AD (2014) **Chemokines in cancer** *Cancer Immunol Res* **2**:1125–1131 <https://doi.org/10.1158/2326-6066.CIR-14-0160>

13. Courtois S, Verhaegh G, North S, Luciani M-G, Lassus P, Hibner U, Oren M, Hainaut P (2002) **DeltaN-p53, a natural isoform of p53 lacking the first transactivation domain, counteracts growth suppression by wild-type p53** *Oncogene* **21**:6722–6728 <https://doi.org/10.1038/sj.onc.1205874>
14. Engeland K (2018) **Cell cycle arrest through indirect transcriptional repression by p53: I have a DREAM** *Cell Death Differ* **25**:114–132 <https://doi.org/10.1038/cdd.2017.172>
15. Feng L-Y, Ou Z-L, Wu F-Y, Shen Z-Z, Shao Z-M (2009) **Involvement of a novel chemokine decoy receptor CCX-CKR in breast cancer growth, metastasis and patient survival** *Clin Cancer Res* **15**:2962–2970 <https://doi.org/10.1158/1078-0432.CCR-08-2495>
16. Flaman JM, Waridel F, Estreicher A, Vannier A, Limacher JM, Gilbert D, Iggo R, Frebourg T (1996) **The human tumour suppressor gene p53 is alternatively spliced in normal cells** *Oncogene* **12**:813–818
17. Fornes O *et al.* (2020) **JASPAR 2020: update of the open-access database of transcription factor binding profiles** *Nucleic Acids Res* **48**:D87–D92 <https://doi.org/10.1093/nar/gkz1001>
18. Georges A, L'Hôte D, Todeschini AL, Auguste A, Legois B, Zider A, Veitia RA (2014) **The transcription factor FOXL2 mobilizes estrogen signaling to maintain the identity of ovarian granulosa cells** *Elife* **3** <https://doi.org/10.7554/eLife.04207>
19. Graubert TA *et al.* (2012) **Recurrent mutations in the U2AF1 splicing factor in myelodysplastic syndromes** *Nat Genet* **44**:53–57 <https://doi.org/10.1038/ng.1031>
20. Hamard P-J *et al.* (2013) **The C terminus of p53 regulates gene expression by multiple mechanisms in a target- and tissue-specific manner in vivo** *Genes Dev* **27**:1868–1885 <https://doi.org/10.1101/gad.224386.113>
21. Haupt S, Caramia F, Herschtal A, Soussi T, Lozano G, Chen H, Liang H, Speed TP, Haupt Y (2019) **Identification of cancer sex-disparity in the functional integrity of p53 and its X chromosome network** *Nat Commun* **10** <https://doi.org/10.1038/s41467-019-13266-3>
22. Hou T, Liang D, Xu L, Huang X, Huang Y, Zhang Y (2013) **Atypical chemokine receptors predict lymph node metastasis and prognosis in patients with cervical squamous cell cancer** *Gynecol Oncol* **130**:181–187 <https://doi.org/10.1016/j.ygyno.2013.04.015>
23. Hummel M *et al.* (2006) **A biologic definition of Burkitt's lymphoma from transcriptional and genomic profiling** *N Engl J Med* **354**:2419–2430 <https://doi.org/10.1056/NEJMoa055351>
24. Ju Y, Sun C, Wang X (2019) **Loss of atypical chemokine receptor 4 facilitates C-C motif chemokine ligand 21-mediated tumor growth and invasion in nasopharyngeal carcinoma** *Exp Ther Med* **17**:613–620 <https://doi.org/10.3892/etm.2018.7007>
25. Knewton KE, Gonzalez Flores JG, Pacicca DM, Robinson JL (2020) **Transcriptome sequencing reveals sex differences in Human meniscal cell response to estrogen based on dosing kinetics (preprint)** *Genomics* <https://doi.org/10.1101/2020.04.27.064451>
26. Lacy SE *et al.* (2020) **Targeted sequencing in DLBCL, molecular subtypes, and outcomes: a Haematological Malignancy Research Network report** *Blood* **135**:1759–1771 <https://doi.org/10.1182/blood.2019003535>

27. Langdon WY, Harris AW, Cory S, Adams JM (1986) **The c-myc oncogene perturbs B lymphocyte development in Eμ-myc transgenic mice** *Cell* **47**:11–18 [https://doi.org/10.1016/0092-8674\(86\)90361-2](https://doi.org/10.1016/0092-8674(86)90361-2)
28. Liao Y, Smyth GK, Shi W (2014) **featureCounts: an efficient general purpose program for assigning sequence reads to genomic features** *Bioinformatics* **30**:923–930 <https://doi.org/10.1093/bioinformatics/btt656>
29. Love MI, Huber W, Anders S (2014) **Moderated estimation of fold change and dispersion for RNA-seq data with DESeq2** *Genome Biol* **15** <https://doi.org/10.1186/s13059-014-0550-8>
30. Lowe SW, Schmitt EM, Smith SW, Osborne BA, Jacks T (1993) **p53 is required for radiation-induced apoptosis in mouse thymocytes** *Nature* **362**:847–849 <https://doi.org/10.1038/362847a0>
31. Mahani A, Arvidsson G, Sadeghi L, Grandien A, Wright APH (2021) **Differential transcriptional reprogramming by wild type and lymphoma-associated mutant MYC proteins as B-Cells convert to a lymphoma phenotype** *Cancers (Basel)* **13** <https://doi.org/10.3390/cancers13236093>
32. Maier B, Gluba W, Bernier B, Turner T, Mohammad K, Guise T, Sutherland A, Thorner M, Scrabble H (2004) **Modulation of mammalian life span by the short isoform of p53** *Genes Dev* **18**:306–319 <https://doi.org/10.1101/gad.1162404>
33. Marcel V *et al.* (2011) **Biological functions of p53 isoforms through evolution: lessons from animal and cellular models** *Cell Death Differ* **18**:1815–1824 <https://doi.org/10.1038/cdd.2011.120>
34. Marcuzzi E, Angioni R, Molon B, Cali B (2018) **Chemokines and Chemokine Receptors: Orchestrating Tumor Metastasis** *Int J Mol Sci* **20** <https://doi.org/10.3390/ijms20010096>
35. Martin M *et al.* (2013) **Exome sequencing identifies recurrent somatic mutations in EIF1AX and SF3B1 in uveal melanoma with disomy 3** *Nat Genet* **45**:933–936 <https://doi.org/10.1038/ng.2674>
36. Mondal AM *et al.* (2013) **p53 isoforms regulate aging- and tumor-associated replicative senescence in T lymphocytes** *J Clin Invest* **123**:5247–5257 <https://doi.org/10.1172/JCI70355>
37. Morin RD *et al.* (2011) **Frequent mutation of histone-modifying genes in non-Hodgkin lymphoma** *Nature* **476**:298–303 <https://doi.org/10.1038/nature10351>
38. Müller A *et al.* (2001) **Involvement of chemokine receptors in breast cancer metastasis** *Nature* **410**:50–56 <https://doi.org/10.1038/35065016>
39. Oki S, Ohta T, Shioi G, Hatanaka H, Ogasawara O, Okuda Y, Kawaji H, Nakaki R, Sese J, Meno C (2018) **Ch IP –Atlas: a data-mining suite powered by full integration of public Ch IP –seq data** *EMBO Rep* **19** <https://doi.org/10.15252/embr.201846255>
40. Pajares MJ, Ezponda T, Catena R, Calvo A, Pio R, Montuenga LM (2007) **Alternative splicing: an emerging topic in molecular and clinical oncology** *Lancet Oncol* **8**:349–357 [https://doi.org/10.1016/S1470-2045\(07\)70104-3](https://doi.org/10.1016/S1470-2045(07)70104-3)
41. Peugeot S, Selivanova G (2021) **p53-Dependent Repression: DREAM or Reality?** *Cancers* **13** <https://doi.org/10.3390/cancers13194850>

42. Qin S, Li B, Li R, Cai Y, Zheng K, Huang H, Xiao F, Zeng M, Xu X (2021) **Proteomic characteristics and identification of PM2.5-induced differentially expressed proteins in hepatocytes and c-Myc silenced hepatocytes** *Ecotoxicol Environ Saf* **209** <https://doi.org/10.1016/j.ecoenv.2020.111838>
43. Rehm A, Mensen A, Schradi K, Gerlach K, Wittstock S, Winter S, Büchner G, Dörken B, Lipp M, Höpken UE (2011) **Cooperative function of CCR7 and lymphotoxin in the formation of a lymphoma-permissive niche within murine secondary lymphoid organs** *Blood* **118**:1020–1033 <https://doi.org/10.1182/blood-2010-11-321265>
44. Senturk S *et al.* (2014) **p53 $\Psi$  is a transcriptionally inactive p53 isoform able to reprogram cells toward a metastatic-like state** *Proc Natl Acad Sci USA* **111**:E3287–96
45. Sette C, Paronetto MP (2022) **Somatic Mutations in Core Spliceosome Components Promote Tumorigenesis and Generate an Exploitable Vulnerability in Human Cancer** *Cancers* **14** <https://doi.org/10.3390/cancers14071827>
46. Shi J-Y *et al.* (2015) **CC chemokine receptor-like 1 functions as a tumour suppressor by impairing CCR7-related chemotaxis in hepatocellular carcinoma: CCRL1 inhibits HCC progression** *J Pathol* **235**:546–558 <https://doi.org/10.1002/path.4450>
47. Si M, Lang J (2018) **The roles of metallothioneins in carcinogenesis** *J Hematol Oncol* **11** <https://doi.org/10.1186/s13045-018-0645-x>
48. Simeonova I *et al.* (2013) **Mutant mice lacking the p53 C-terminal domain model telomere syndromes** *Cell Rep* **3**:2046–2058 <https://doi.org/10.1016/j.celrep.2013.05.028>
49. Simeonova I, Lejour V, Bardot B, Bouarich-Bourimi R, Morin A, Fang M, Charbonnier L, Toledo F (2012) **Fuzzy Tandem Repeats Containing p53 Response Elements May Define Species-Specific p53 Target Genes** *PLoS Genet* **8** <https://doi.org/10.1371/journal.pgen.1002731>
50. Slatter TL, Ganesan P, Holzhauer C, Mehta R, Rubio C, Williams G, Wilson M, Royds JA, Baird MA, Braithwaite AW (2010) **p53-mediated apoptosis prevents the accumulation of progenitor B cells and B-cell tumors** *Cell Death Differ* **17**:540–550 <https://doi.org/10.1038/cdd.2009.136>
51. Steffens Reinhardt L, Zhang X, Wawruszak A, Groen K, De Iuliis GN, Avery-Kiejda KA (2020) **Good Cop, Bad Cop: Defining the Roles of  $\Delta 40p53$  in Cancer and Aging** *Cancers (Basel)* **12** <https://doi.org/10.3390/cancers12061659>
52. Toledo F, Krummel KA, Lee CJ, Liu C-W, Rodewald L-W, Tang M, Wahl GM (2006) **A mouse p53 mutant lacking the proline-rich domain rescues Mdm4 deficiency and provides insight into the Mdm2-Mdm4-p53 regulatory network** *Cancer Cell* **9**:273–285 <https://doi.org/10.1016/j.ccr.2006.03.014>
53. Tress ML, Abascal F, Valencia A (2017) **Alternative Splicing May Not Be the Key to Proteome Complexity** *Trends Biochem Sci* **42**:98–110 <https://doi.org/10.1016/j.tibs.2016.08.008>
54. Tress ML, Abascal F, Valencia A (2017) **Most Alternative Isoforms Are Not Functionally Important** *Trends Biochem Sci* **42**:408–410 <https://doi.org/10.1016/j.tibs.2017.04.002>
55. Ule J, Blencowe BJ (2019) **Alternative Splicing Regulatory Networks: Functions, Mechanisms, and Evolution** *Molecular Cell* **76**:329–345 <https://doi.org/10.1016/j.molcel.2019.09.017>

56. Ulvmar MH *et al.* (2014) **The atypical chemokine receptor CCRL1 shapes functional CCL21 gradients in lymph nodes** *Nat Immunol* **15**:623–630 <https://doi.org/10.1038/ni.2889>
57. Vassilev LT *et al.* (2004) **In vivo activation of the p53 pathway by small-molecule antagonists of MDM2** *Science* **303**:844–848 <https://doi.org/10.1126/science.1092472>
58. Weatheritt RJ, Sterne-Weiler T, Blencowe BJ (2016) **The ribosome-engaged landscape of alternative splicing** *Nat Struct Mol Biol* **23**:1117–1123 <https://doi.org/10.1038/nsmb.3317>
59. Yin Y, Stephen CW, Luciani MG, Fåhræus R (2002) **p53 Stability and activity is regulated by Mdm2-mediated induction of alternative p53 translation products** *Nat Cell Biol* **4**:462–467 <https://doi.org/10.1038/ncb801>
60. Younger ST, Kenzelmann-Broz D, Jung H, Attardi LD, Rinn JL (2015) **Integrative genomic analysis reveals widespread enhancer regulation by p53 in response to DNA damage** *Nucleic Acids Res* **43**:4447–4462 <https://doi.org/10.1093/nar/gkv284>
61. Zhu Q, Chen H, Li X, Wang X, Yan H (2022) **JMJD2C mediates the MDM2/p53/IL5RA axis to promote CDDP resistance in uveal melanoma** *Cell Death Discov* **8** <https://doi.org/10.1038/s41420-022-00949-y>
62. Zhu Y, Tang W, Liu Y, Wang G, Liang Z, Cui L (2014) **CCX-CKR expression in colorectal cancer and patient survival** *Int J Biol Markers* **29**:e40–48 <https://doi.org/10.5301/jbm.5000057>

## Article and author information

### Anne Fajac

Genetics of Tumor Suppression, Institut Curie, Paris, 75248 Cedex 05, France, CNRS UMR3244, Paris, France, Sorbonne University, Paris, France, PSL Research University, Paris, France

### Iva Simeonova

Genetics of Tumor Suppression, Institut Curie, Paris, 75248 Cedex 05, France, CNRS UMR3244, Paris, France, Sorbonne University, Paris, France, PSL Research University, Paris, France

### Julia Leemput

Genetics of Tumor Suppression, Institut Curie, Paris, 75248 Cedex 05, France, CNRS UMR3244, Paris, France, Sorbonne University, Paris, France, PSL Research University, Paris, France

### Marc Gabriel

CNRS UMR3244, Paris, France, Sorbonne University, Paris, France, PSL Research University, Paris, France, Non Coding RNA, Epigenetic and Genome Fluidity, Institut Curie, Paris, France

### Aurélie Morin

Genetics of Tumor Suppression, Institut Curie, Paris, 75248 Cedex 05, France, CNRS UMR3244, Paris, France, Sorbonne University, Paris, France, PSL Research University, Paris, France

### Vincent Lejour

Genetics of Tumor Suppression, Institut Curie, Paris, 75248 Cedex 05, France, CNRS UMR3244, Paris, France, Sorbonne University, Paris, France, PSL Research University, Paris, France

**Annaïg Hamon**

Genetics of Tumor Suppression, Institut Curie, Paris, 75248 Cedex 05, France, CNRS UMR3244, Paris, France, Sorbonne University, Paris, France, PSL Research University, Paris, France

**Wilhelm Vaysse-Zinkhöfer**

Genetics of Tumor Suppression, Institut Curie, Paris, 75248 Cedex 05, France, CNRS UMR3244, Paris, France, Sorbonne University, Paris, France, PSL Research University, Paris, France

**Eliana Eldawra**

Genetics of Tumor Suppression, Institut Curie, Paris, 75248 Cedex 05, France, CNRS UMR3244, Paris, France, Sorbonne University, Paris, France, PSL Research University, Paris, France

**Jeanne Rakotopare**

Genetics of Tumor Suppression, Institut Curie, Paris, 75248 Cedex 05, France, CNRS UMR3244, Paris, France, Sorbonne University, Paris, France, PSL Research University, Paris, France

**Marina Pinskaya**

CNRS UMR3244, Paris, France, Sorbonne University, Paris, France, PSL Research University, Paris, France, Non Coding RNA, Epigenetic and Genome Fluidity, Institut Curie, Paris, France  
ORCID iD: [0000-0003-1992-0264](https://orcid.org/0000-0003-1992-0264)

**Antonin Morillon**

CNRS UMR3244, Paris, France, Sorbonne University, Paris, France, PSL Research University, Paris, France, Non Coding RNA, Epigenetic and Genome Fluidity, Institut Curie, Paris, France  
ORCID iD: [0000-0002-0575-5264](https://orcid.org/0000-0002-0575-5264)

**Jean-Christophe Bourdon**

Ninewells Hospital, University of Dundee, Dundee 19SY, Scotland  
ORCID iD: [0000-0003-4623-9386](https://orcid.org/0000-0003-4623-9386)

**Boris Bardot**

Genetics of Tumor Suppression, Institut Curie, Paris, 75248 Cedex 05, France, CNRS UMR3244, Paris, France, Sorbonne University, Paris, France, PSL Research University, Paris, France  
**For correspondence:** [boris.bardot@curie.fr](mailto:boris.bardot@curie.fr)

**Franck Toledo**

Genetics of Tumor Suppression, Institut Curie, Paris, 75248 Cedex 05, France, CNRS UMR3244, Paris, France, Sorbonne University, Paris, France, PSL Research University, Paris, France  
**For correspondence:** [franck.toledo@curie.fr](mailto:franck.toledo@curie.fr)  
ORCID iD: [0000-0003-3798-4106](https://orcid.org/0000-0003-3798-4106)

**Copyright**

© 2024, Fajac et al.

This article is distributed under the terms of the [Creative Commons Attribution License](https://creativecommons.org/licenses/by/4.0/), which permits unrestricted use and redistribution provided that the original author and source are credited.



## Editors

Reviewing Editor

**Yamini Dalal**

National Cancer Institute, Bethesda, United States of America

Senior Editor

**Yamini Dalal**

National Cancer Institute, Bethesda, United States of America

### Reviewer #1 (Public Review):

Summary:

The authors originally investigated the function of p53 isoforms with an alternative C-terminus encoded by the Alternatively Spliced (AS) exon in place of exon 11 encoding the canonical "α" C-terminal domain. For this purpose, the authors create a mouse model with a specific deletion of the AS exon.

Strengths:

Interestingly, wt or p53 $\Delta$ AS/ $\Delta$ AS mouse embryonic fibroblasts did not differ in cell cycle control, expression of well-known p53 target genes, proliferation under hyperoxic conditions, or the growth of tumor xenografts. However, p53-AS isoforms were shown to confer male-specific protection against lymphomagenesis in E $\mu$ -Myc transgenic mice, prone to highly penetrant B-cell lymphomas. In fact, p53 $\Delta$ AS/ $\Delta$ AS E $\mu$ -Myc mice were less protected from developing B-cell lymphomas compared to WT counterparts. The important difference that the authors find between WT and p53 $\Delta$ AS/ $\Delta$ AS E $\mu$ -Myc males is a higher number of immature B cells in p53 $\Delta$ AS/ $\Delta$ AS vs WT mice. Higher expression of Akr4 and lower expression of Mt2 was found in p53 $^{+/-}$  E $\mu$ -Myc males compared to p53 $\Delta$ AS/ $\Delta$ AS counterparts, suggesting that these two transcripts are in part regulators of B-cell lymphomagenesis and enrichment for immature B cells.

Weaknesses:

The manuscript is interesting but the data are not so striking and are very correlative. The authors should add functional experiments to reinforce their hypotheses and to provide, beyond potential prognostic factors, any potential mechanism at the basis of the different rates of B-cell lymphomagenesis in males vs females individuals and in WT vs p53 $\Delta$ AS/ $\Delta$ AS E $\mu$ -Myc males.

- <https://doi.org/10.7554/eLife.92774.1.sa1>

### Reviewer #2 (Public Review):

Summary:

This manuscript provides a detailed analysis of B-cell lymphomagenesis in mice lacking an alternative exon in the region encoding the C-terminal (regulatory) domain of the p53 protein and thus enable to assemble the so-called p53AS isoform. This isoform differs from canonical p53 by the replacement of roughly 30 c-terminal residues by about 10 residues encoded by the alternative exon. There is biochemical and biological evidence that p53AS retains strong transcriptional and somewhat enhanced suppressive activities, with mouse models expressing protein constructs similar to p53AS showing signs of increased p53 activity leading to rapid and lethal anemia. However, the precise role of the alternative p53AS variant has not been addressed so far in a mouse model aimed at demonstrating whether the lack of this particular p53 isoform (trp53 $\Delta$ AS/ $\Delta$ AS mice) may cause a specific pathological phenotype.

Results show that lack of AS expression does not noticeably affect p53 transcriptional activity but reveals a subtle pathogenic phenotype, with trp53 $\Delta$ AS/ $\Delta$ AS males, but not females,

tending to develop more frequently and earlier B-cell lymphoma than WT. Next, the authors then introduced  $\Delta$ AS in transgenic E $\mu$ -Myc mice that show accelerated lymphomagenesis. They show that lack of AS caused increased lethality and larger tumor lymph nodes in p53 $\Delta$ AS E $\mu$ -Myc males compared to their p53WT E $\mu$ -Myc male counterparts, but not in females. Comparative transcriptomics identified a small set of candidate, differentially expressed genes, including Akr4 (atypical chemokine receptor 4), which was significantly less expressed in the spleens of  $\Delta$ AS compared to WT controls. Akr4 encodes a dummy receptor acting as an interceptor for multiple chemokines and thus may negatively regulate a chemokine/cytokine signalling axis involved in lymphomagenesis, which is down-regulated by estrogen signalling. Using in vitro cell models, the authors provide evidence that Akr4 is a transcriptional target for p53 and that its p53-dependent activation is repressed by 17 $\beta$ -oestradiol. Finally, seeking evidence for a relevance for this gene in human lymphomagenesis, the authors analyse Burkitt lymphoma transcriptomic datasets and show that high ACKR4 expression correlated with better survival in males, but not in females

#### Strengths:

A convincing demonstration of a subtle, gender-specific pathogenic phenotype associated with the lack of p53AS. The characterization of trp53 $\Delta$ AS/ $\Delta$ AS is well described and the data presented are convincing. This represents a significant achievement since, as mentioned, in vivo data establishing the relevance of p53AS isoform remains scarce. Based on this initial observation, the authors provide strong correlative evidence that this particular phenotype is associated by differential expression of Akr4.

#### Weaknesses:

The study does not demonstrate how p53AS may specifically and differentially contribute to the regulation of Akr4, nor whether restoring Akr4 expression may nullify the observed phenotype.

- <https://doi.org/10.7554/eLife.92774.1.sa0>